

LAPPEENRANTA-LAHTI UNIVERSITY OF TECHNOLOGY LUT
School of Energy Systems
Degree Programme in Energy Technology

Matias Pessa

**FOULING AND CLEANING OF WASTE HEAT RECOVERY BOILERS AFTER
LIQUID FIRED MEDIUM SPEED RECIPROCATING ENGINES**

Examiners: Professor, D.Sc. (Tech.) Esa Vakkilainen
M.Sc. (Tech.) Matti Takasuo

ABSTRACT

Lappeenranta-Lahti University of Technology LUT
School of Energy Systems
Degree Programme in Energy Technology

Matias Pessa

Fouling and cleaning of waste heat recovery boilers after liquid fired medium speed reciprocating engines

Master's thesis
2020

65 pages, 28 figures and 4 tables.

Examiners: Professor, D.Sc. (Tech.) Esa Vakkilainen and M.Sc. (Tech.) Matti Takasuo

Keywords: exhaust gas, fouling, heat recovery, reciprocating engine, soot blower, soot blowing, waste heat recovery boiler

This thesis studies fouling and cleaning of waste heat recovery boilers after liquid fired medium speed reciprocating engines. Fouling has a large effect on the performance of waste heat recovery boilers. The theory part of this thesis explains the basics of boiler heat transfer, fouling and on-line cleaning methods.

In the experimental part of the thesis waste heat recovery boilers situated in an engine power plant in Asia are studied. The aim of the study was to find out the effect of fouling and cleaning on the boiler performance. This was done by conducting measurements on site and analysing the data from plant's logged control system data. The objective was to find a correlation between experienced fouling and boiler performance. The performance and effect of soot blowing was also assessed.

The conclusion from the measured and analysed data was that it was insufficient to determine long-term development of fouling. Suggestion for on-line measurement have been done to generate data from a longer period of time. Soot blower performance was deemed good and suggestions were made to preserve steam. Only dispense steam on the return stroke of the soot blower and to install an acoustic soot blower.

TIIVISTELMÄ

Lappeenrannan-Lahden teknillinen yliopisto LUT
School of Energy Systems
Energiatekniikan koulutusohjelma

Matias Pessa

Lämmöntalteenottokattilan likaantuminen ja puhdistus nestemäisiä polttoaineita polttavien keskinopeiden mäntämoottoreiden jälkeen

Diplomityö
2020

65 sivua, 28 kuvaa ja 4 taulukkoa.

Tarkastajat: Professori, TkT Esa Vakkilainen ja DI Matti Takasuo

Hakusanat: likaantuminen, lämmöntalteenotto, lämmöntalteenottokattila, mäntämoottori, nuohoin, nuohous, pakokaasu

Tämä opinnäytetyö tutkii lämmöntalteenottokattilan likaantumista ja puhdistusta nestemäisiä polttoaineita polttavien keskinopeiden mäntämoottoreiden jälkeen. Likaantumisella on suuri vaikutus lämmöntalteenottokattilan suorituskykyyn. Työn teoriaosuus selostaa kattilan lämmönsiirron perusteet, likaantumisen ja käytönaikaiset puhdistusmenetelmät.

Työn kokeellisessa osuudessa tutkitaan lämmöntalteenottokattiloita Aasiassa sijaitsevassa moottorivoimalaitoksessa. Tutkimuksen tavoitteena oli selvittää likaantumisen ja nuohouksen vaikutukset kattilan suorituskykyyn. Tätä varten laitoksella tehtiin mittauksia ja tutkittiin laitoksen ohjausjärjelmän tallentamaa dataa. Tavoitteena oli löytää yhteys likaantumisen ja kattilan suorituskyvyn väliltä. Nuohointen suorituskyky ja vaikutus selvitettiin.

Mitatun ja analysoidun datan perusteella todettiin sen olevan riittämätön pitkän ajan likaantumisen kehittymisen arvioimiseen. Ehdotuksena annettiin datan etäluentajärjestelmä, jolla voidaan varmistaa datan saanti tarvittavan pitkältä ajalta. Nuohointen teho todettiin hyväksi ja sen perusteella annettiin suositukset höyryn säästämiseksi. Höyryä tulisi syöttää ainoastaan nuohoinen takaisinvedon aikana ja kattilaan voitaisiin asentaa akustinen nuohoin.

ACKNOWLEDGEMENTS

This thesis has been done as a commission of Alfa Laval Aalborg Oy, Rauma.

I would like to thank my supervisor M.Sc. (Tech.) Matti Takasuo for having time to help me when needed. I would also like to thank my examiner Professor, D.Sc. (Tech.) Esa Vakkiainen for his support. I would also like to thank my superior at Alfa Laval Aalborg, Pekka Läiskä for providing an inspiring and challenging workplace, not to forget all my great colleagues at Business Development.

Special thanks to Saunalenkki for the fun times during our studies and the friendship that has continued ever since.

I would also like to express my gratitude to my family for their support through my studies.

Finally, I would like to thank fiancé Anna – sometimes tough love is needed.

Rauma 7.12.2020



Matias Pessa

TABLE OF CONTENTS

ABSTRACT

TIIVISTELMÄ

ACKNOWLEDGEMENTS

TABLE OF CONTENTS

LIST OF SYMBOLS AND ABBREVIATIONS

1	INTRODUCTION	10
1.1	Objectives	10
1.2	Outline	10
2	WASTE HEAT RECOVERY IN ENGINE POWER PLANTS	12
2.1	Reciprocating internal combustion engine	14
2.2	Waste heat recovery applications	15
3	WASTE HEAT RECOVERY BOILERS	19
3.1	Waste heat recovery boiler	19
4	FOULING	26
4.1	History of fouling models	26
4.2	Fouling mechanisms	27
4.2.1	Particle inertial impaction	28
4.2.2	Thermophoresis	28
4.2.3	Brownian motion	28
4.2.4	Turbulent eddy impaction	29
5	CLEANING OF HEATING SURFACES	30
5.1	Steam soot blowing	31
5.1.1	Rake steam soot blower	34
5.1.2	Rotating steam soot blower	36
5.1.3	Downsides of steam soot blowing - erosion	37
5.2	Compressed air soot blowing	40

5.3	Water soot blowing.....	41
5.4	Acoustic soot blowing	41
6	CASE STORY: ECC PLANT IN SOUTH ASIA	47
7	RESEARCH METHODS	48
7.1	Measurements	48
7.1.1	WHRB steam flow before and after soot blowing	48
7.1.2	Soot layer thickness measurement and visual inspection.....	50
8	RESULTS	52
8.1	Effect of soot blowing on WHRB output	52
8.2	Soot layer thickness measurements and visual observations.....	53
8.3	Data analysis from control system's logged data	54
9	DISCUSSION	55
9.1	Soot layer thickness measurements and visual inspection	55
9.2	Long-term performance based on plant's logged control system data	56
9.3	Soot blowers	57
10	CONCLUSIONS	59
	REFERENCES	60

LIST OF SYMBOLS AND ABBREVIATIONS

Roman

A	area	m^2
a	speed of sound	m/s
c_p	specific heat capacity at constant pressure	kJ/kgK
CF	cleanliness factor	-
d	diameter	m
D	diameter	m
F	cross flow correction factor	-
h	convection heat transfer coefficient	$\text{W/m}^2\text{K}$
h	specific enthalpy	kJ/kg
k	thermal conductivity	W/mK
L	thickness	m
\dot{m}	mass flow	kg/s, kg/h
p	pressure	bar
P	power	W
q	heat transfer rate	W
q''	heat flux	W/m^2
R	thermal resistance	$\text{m}^2\text{K/W}$
T	temperature	$^{\circ}\text{C}$
U	overall heat transfer coefficient	$\text{W/m}^2\text{K}$
v	velocity	m/s

Greek

α	absorptivity	-
ε	emissivity	-
η	efficiency	-
μ	dynamic viscosity	kg/ms
ρ	density	kg/m^3
σ	Stefan-Boltzmann constant	$\text{W/m}^2\text{K}$

Dimensionless numbers

M	Mach number
Stk	Stokes number

Subscripts

c	cold
cond	conductive
conv	convective
e	electric
eg	exhaust gas
f	fin
f	fouling
g	gas
h	hot
in	inlet
lm	logarithmic mean
loss	loss
o	overall
out	outlet
net	net
rad	radiation
s	surface
s	steam
sup	superheated
sur	surrounding
w	wall
∞	fluid

Abbreviations

CFD	Computational Fluid Dynamics
CHP	Combined Heat and Power
ECC	Engine Combined Cycle
GT	Gas Turbine

HFO	Heavy Fuel Oil
LBF	Liquid Bio Fuel
NWL	Normal Water Level
ORC	Organic Rankine Cycle
PIP	Peak Impact Pressure
RICE	Reciprocating Internal Combustion Engine
SC	Simple Cycle
STG	Steam Turbine Generator
WHRB	Waste Heat Recovery Boiler

1 INTRODUCTION

The world is moving to a constantly more energy efficient direction, where efficiency optimization is done across all fields. The driver being increasingly also about reducing emissions and greenhouse gases instead of done solely from a financial perspective. Waste heat recovery applications are used nowadays increasingly across different industries and applications to increase the efficiency of any given system. Higher efficiency reduces fuel consumption and carbon dioxide (CO₂) emissions from applications involving any sort of combustion.

Alfa Laval Aalborg Oy sells, designs and manufactures waste heat recovery system mostly to industrial and power generation application, such as reciprocating engines and gas turbines. In this thesis waste heat recovery boilers with extended heating surfaces designed after liquid fired medium speed reciprocating engines are investigated. The exhaust gases from liquid reciprocating engines are not clean combustion gases but contain particles. Understanding the effect of fouling and cleaning, and their impact on boiler design is at utmost importance to design effective boilers from both performance and financial perspective.

1.1 Objectives

The main objective of this thesis is to answer the question how to establish a correlation of the effect of heating surface fouling in waste heat recovery boilers after liquid fired medium speed reciprocating engines. This is done by performing both empirical on-line measurements in a power plant as well as analysing the long-time data saved by the power plant's logged control system data. The gathered data is then compared to analytical calculations to understand fouling over time. Secondly, to find out how the effect of soot blowing in long time performance and if improvement can be made to the case story power plant.

1.2 Outline

Chapter 1 introduces the background, motivation, objectives and outline of the thesis. Chapter 2 introduces basics of engine power plants and different waste heat recovery solutions in plants. Chapter 3 introduces general principle of waste heat recovery boilers and related heat transfer aspects. Chapter 4 discusses fouling mechanism and models. Chapter 5 introduces

different methods for on-line cleaning of heating surfaces. Chapter 6 describes the engine power plant where measurements were done. Chapter 7 outlines the measurements. Chapter 8 presents the results. Chapter 9 contains the discussion part of the thesis. Chapter 10 conclusions are summarized and further recommendations are given based on the thesis.

2 WASTE HEAT RECOVERY IN ENGINE POWER PLANTS

Reciprocating internal combustion engines (RICE) cover 10–15% of the world's power demand. They are used for various purposes ranging from typical power generation to some niche economy sectors e.g. remote locations not connected to the grid, due to their fuel economy, sturdiness, multiple redundant units and flexibility. Engines are used as prime movers for combined heat & power (CHP) and power generation such as backup, standby/emergency, grid stabilization, peaking and base load plants. (Adefarati et al. 2017, 70–71.)

CHP plants, which in addition to electric power generate heat to be used for industrial processes or district heating. These plants are typically running only during the heating season, unless they are so-called trigeneration plant's that convert the generated heat to cooling with chillers. A good example is Germany, where multiple engine-based CHP plants have been built in the past years. The country's Combined Heat and Power Act was revised in January 2016, and since then 200 MW_e have been auctioned each year with fixed feed tariff basis (Federal Ministry for Economic Affairs and Energy).

Engines are commonly used as standby/emergency generator in facilities and systems which are infrastructurally important utilities such as hospitals, data centres and telecommunication equipment. The yearly running hours for standby/emergency generators are so limited that they are not implemented with any waste heat recovery. These units can even be limited by their permit to be used solely for emergency purposes rather than other power generation purposes. (EPA 2017, 2-3.)

Peak shaving units are used by facilities to produce electricity to their own purposes during electrical consumption peaks. This means that the plant is owned by the actual consumer rather than local utility. Typical arrangement is that the utility will ask the facility to run its peak shaving engines during high peaks and in exchange provide monthly payments for this service (EPA 2017, 2-3).

In traditional power generation the engine plants can be divided to base load plants and peaking plants, but with today's emerging renewables, wind and solar, hardly any can be classified as base load plants anymore. Grid stabilization is done by both types of engines

not just peaking plants. Engine power plants typically compete within the same segment as gas turbines (GT) in power generation. Below Figure 1 shows the efficiency of engine and GT plants.

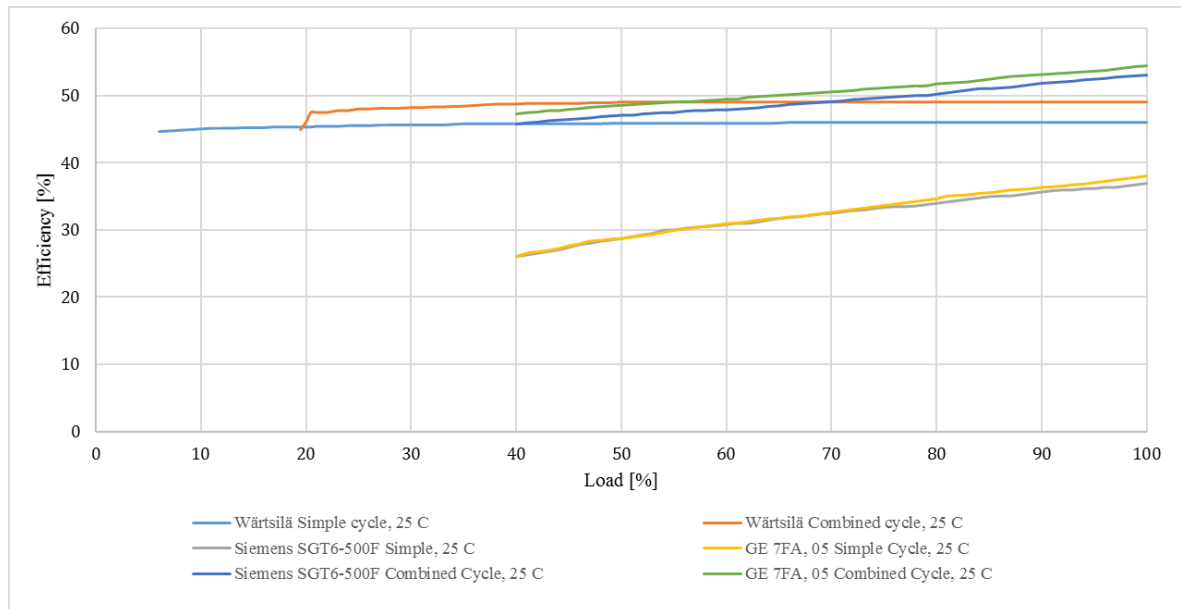


Figure 1. Engine vs. GT plant efficiencies on different loads in both single and combined cycle (adapted from Wärtsilä 2018).

As seen from above both simple and combined cycle engine plants keep their efficiencies high without any significant decrease throughout the load scale down to 6% and 20% loads, respectively. The turndown of an engine plant is good because it consists of multiple units. Take a 200 MW plant as an example, it consists of e.g. 11 x 18 MW_e engines where a similar size GT plant would consist only of one or two units.

In Figure 1 it can be observed that GT plant's efficiency drop is much steeper compared to engine plant's curves. The GTs also go only down to 40% load, which is the minimum emissions-compliant load. Meaning lower loads than that do not fulfil the environmental emission limits anymore (Wärtsilä 2018). Taking this into account and the fact that few power plants between 50–250 MW_e are running on their optimal 100% load continuously i.e. base load. The power generation is shifting towards engines in the future especially in CHP, base load and peaking power plants. (Delta-EE 2017.)

2.1 Reciprocating internal combustion engine

RICEs can be divided to Otto- and Diesel-cycles, based on their ignition method. The engines can also be classified by their running speed to high speed 1000–3600 rpm, medium speed 275–1000 rpm and low speed engines 58–275 rpm. Lastly the engines can be divided to 2-stroke and 4-stroke engines by their operating cycle. (Adefarati et al. 2017, 76–80.) Engine sizes in power generation typically vary from 10 kW to 18 MW, however low speed 2-stroke are available up to 84 MW but are more commonly used in marine propulsion systems rather than power generation (EPA 2017, 2-1; 2-13).

The engines are defined by their ignition method. In the Otto-cycle the fuel-air mixture is ignited by a spark plug. Spark ignited engines are capable of running on a wide range of fuels that are difficult to ignite with compression. Gas fired spark ignited engines typically result in lower emissions than diesel engines which has increased their popularity when investment decisions are made with environmental aspects in mind as well. In diesel engines the ignition is done by the compressed hot air, and no external ignition is needed. (Adefarati et al. 2017, 76.)

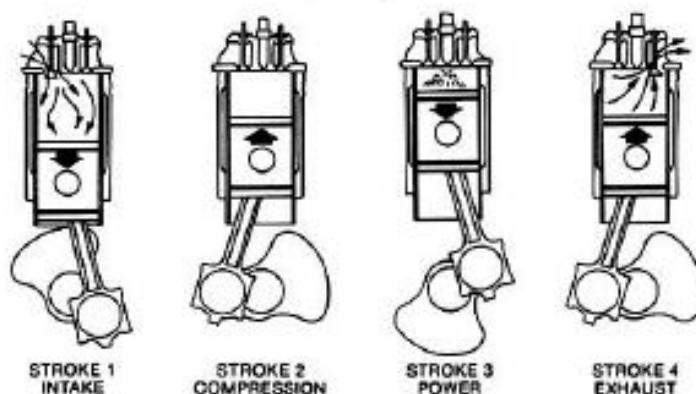


Figure 2. 4-stroke power cycle of the piston within cylinder (EPA 2017, 4).

The 4-stroke cycle which is more common can be separated into 4 different strokes:

- 1) Intake stroke – Air (diesel) or fuel-air mixture (spark ignited) to cylinder.
- 2) Compression stroke – Air or fuel-air mixture is compressed within the cylinder. In a diesel engine the fuel is injected near the end of the compression where it is ignited by the high temperature of the compressed air. In a spark ignition engine the fuel-air mixture is ignited by the spark plug near the end of compression.

- 3) Power stroke – The piston is expanded by the hot and high pressure combustion gases.
- 4) Exhaust stroke – The exhaust gases are pushed out of the cylinder through exhaust port. (EPA 2017,4.)

2.2 Waste heat recovery applications

The energy recovered from the RICE exhaust gases can be utilized for several purposes using different media, but the common nominator for all solutions is to increase power plant's total efficiency. Typical media include water/steam, thermal oil, water-glycol mixture but also new emerging technologies are being investigated such as supercritical carbon dioxide (S-CO₂) (Kim et al. 2017, 893). This thesis focuses on the conventional steam/water medium.

As its simplest waste heat recovery is used in simple cycle (SC) power plants when using heavy fuel oil (HFO). Heat is recovered from exhaust gases to be used to heat HFO tanks, separators, booster units and transfer line. Otherwise the heating would be done with electrical heaters which would increase plant's auxiliary power consumption resulting in lower electrical net output or a fired unit that would increase total fuel consumption.

Another typical waste heat recovery application is CHP, where recovered heat is used outside the power plant by different consumers. Typical usages are process steam, district heating or cooling using absorption chillers. By maximizing the heat recovery from engine exhaust gases as well as engine's cooling water circuits plant efficiencies over 90% are achievable, as shown in Figure 3.

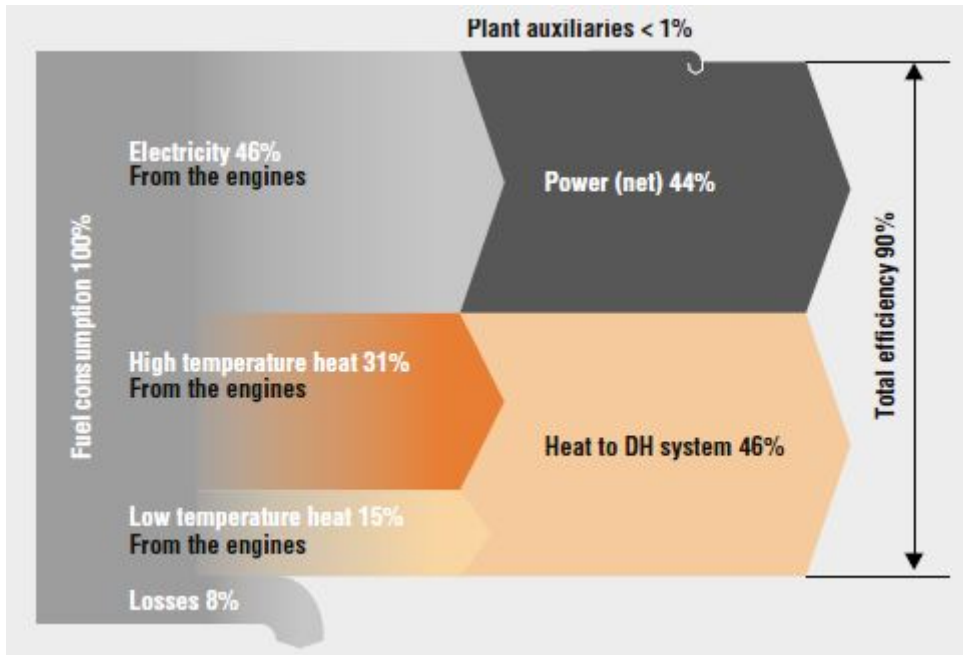


Figure 3. Energy balance of RICE for a district heating system shown as a Sankey-diagram (Wärtsilä 2017).

Lastly, when additional electricity is required from an engine power plant it can be utilized in a combined cycle plant, namely an Engine Combined Cycle (ECC) plant. Where steam, produced by waste heat recovery boilers (WHRB) recovering heat from the engine exhaust gases, is used in steam turbine generator (STG) to produce electricity. A typical ECC layout along its main equipment shown below in Figure 4.

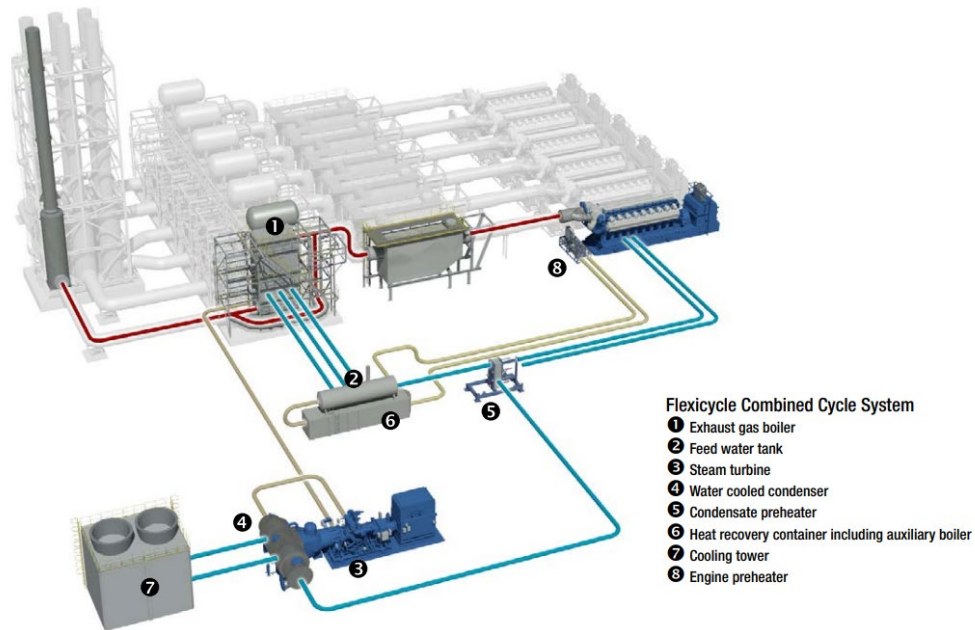


Figure 4. Typical ECC power plant (Wärtsilä 2015).

A steam based combined cycle is called Rankine cycle. Typically, in engine power plants a combined cycle raises the plant's electrical output by 6–10%. The available exhaust gas temperatures from engine vary between 300–400°C, on partial loads the temperatures can go up to 450°C but engines are however typically ran on the optimal efficiency. Due to relatively low temperature levels compared to gas turbines and large fired boilers, the pressure and temperature levels for superheated steam are relatively low. Typical operating parameters for ECC steam cycles are pressures of 10–30 bars with superheating temperatures between 280–380°C depending on exhaust gas temperature and STG selection.

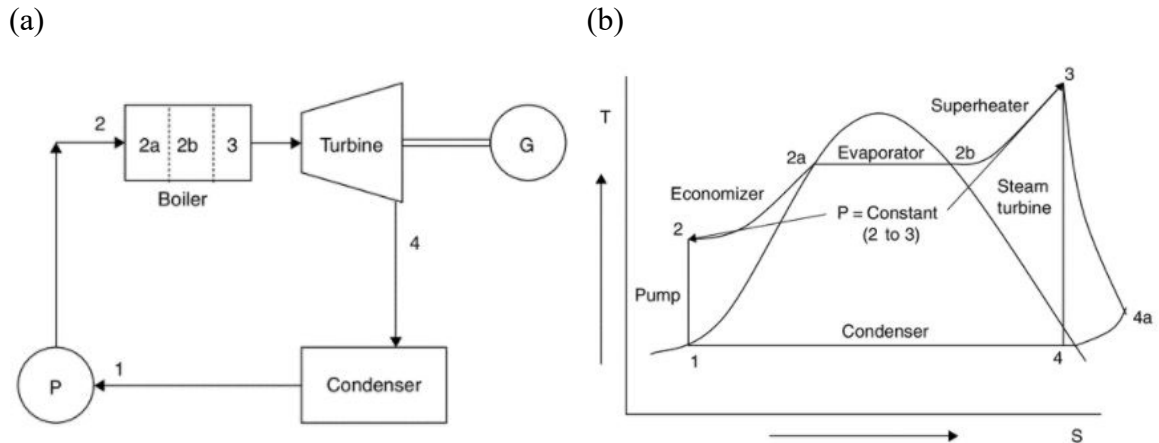


Figure 5. (a) Typical flow diagram of a steam turbine plant, where 2a is economizer, 2b is evaporator, 3 is superheater, P is pump and G is generator (Rao 2012, 13). (b) The same steam turbine plant shown in an ideal T,s -diagram, where T is temperature and s is entropy. The hill shaped curve shows the state of water, where left side is liquid state, middle is water-steam mixture (wet steam) and right side is dry steam (modified from Rao 2012, 14).

The basic principle of Rankine cycle is shown above. The operation principle is as follows

1→2 Water is pressurized up to boiler operating pressure with a pump. **2→2a** Pressurized water is heated up to saturation temperature in the economizer. **2a→2b** Saturated water is evaporated to saturated steam in the evaporator. **2b→3** Saturated steam is superheated in the superheater. **3→4(a)** Superheated steam is expanded in the steam turbine to a lower pressure and temperature. 4 shows isentropic expansions and 4a real expansion. **4(a)→1** Steam is condensed in the condenser. The steam is often superheated to increase its enthalpy and to avoid turbine blade erosion due to water droplets.

Another emerging bottoming cycle is Organic Rankine Cycle (ORC), which as the name states is based on the Rankine Cycle but uses organic fluid as a medium instead of water/steam.

3 WASTE HEAT RECOVERY BOILERS

Waste heat recovery boilers (WHRB) are used in different applications to recover heat from hot flue gases by transferring the heat to another medium that can then be used for various processes as outlined in 2.2. This chapter first describes the construction and basic operation of a water tube WHRB meant for heat recovery from engine exhaust gases.

3.1 Waste heat recovery boiler

A WHRB can be of water tube or smoke tube type. In a water tube boiler the water flows inside the tubes which are situated in the flow field of the flue gases and/or in the side walls as a membrane wall construction. The water tube boiler is suitable for high pressures as the diameter of the tubes is rather small. The water tube construction is scalable for different constructions and flow quantities, and with extended heating surfaces the even for high recovery rates are compact. The water tube design also allows easily multiple heating sections within the same boiler. Water tube boilers can be divided to natural circulation, forced circulation and once-through boilers. Natural circulation is based on the density difference between saturated water in the downcomer and saturated water-steam mixture in the boiler tubes and riser, basic flow diagram can be seen from Figure 6. Forced circulation is similar as natural circulation but has a pump in the downcomer to create the required driving force for circulation. The downside of forced circulation is the electricity consumption or required maintenance of the pump. Once-through boilers are designed so that all feed water fed to the boiler gets evaporated to steam and possibly superheated before boiler outlet, so there are no steam drum to separate the water-steam mixture like in natural and forced circulation boilers. (Vakkilainen 2016, 89–93.)

In a smoke tube boiler the exhaust gas flows inside the tubes which are surrounded by water in the pressure vessel, hence it is not suitable for high pressures. The heat transfer rate of the smoke tube inside the tubes is low, so it is used mostly in medium or low heat recovery demands as with low pinch points the size quickly becomes large.

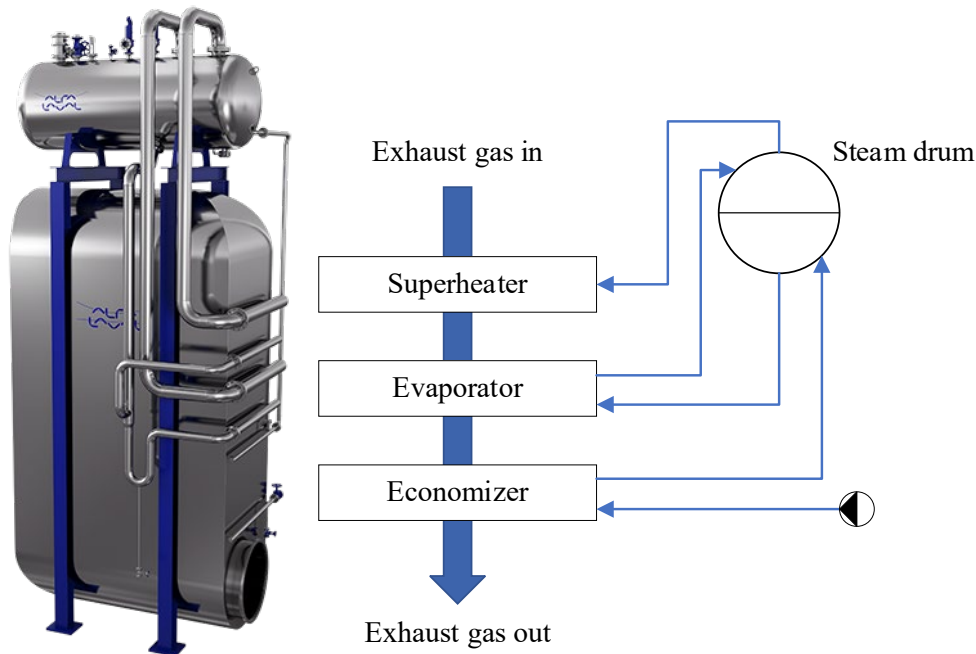


Figure 6. Alfa Laval Aalborg AV-6N waste heat recovery boiler (Alfa Laval Aalborg Oy, 2020) with typical flow scheme of a natural circulation waste heat recovery boiler with superheated, evaporator and economizer.

Above we can see a typical construction of a natural circulation WHRB after engine exhaust gases. The exhaust gas is led through different tube bundle sections, namely superheater, evaporator and economizer, and heat is transferred to water/steam from the exhaust gases. The feed water is pumped through the economizer, where its temperature is raised close to saturation, to the steam drum. Within the steam drum the water/steam is in saturated condition clearly separated to two phases, denser water on the bottom and less dense steam on upper part. From the steam drum the saturated water is led via downcomer to the evaporator, where part of water is evaporated into steam. With the density difference created by steam bubbles within water the water-steam mixture is circulated back to the steam drum, where the mixture is separated. After the steam is separated in the steam drum it is led to the superheater where it is superheated. Typically, the upper part of the steam drum contains a demister to make sure there are no droplets of water being carried to the superheated along the dry saturated steam to avoid any dissolved solids to carry over.

WHRBs follow the same physical mechanisms and rules as any other phenomenon, if a temperature difference between media exists heat transfer must happen (Bergman et al. 2011, 2). The heat from the exhaust gases is transferred to the water/steam within the tubes by convection and radiation to the tube surface, further by conduction through the tube wall and

lastly by convection to water/steam. Convection is heat transfer caused by movement of fluid by a surface. Convective heat transfer consists of two phenomena, random molecular motion of the fluid, also called diffusion, and bulk motion of the fluid at the boundary layer. The equation for convective heat flux can be written as follows

$$q''_{\text{conv}} = h(T_{\infty} - T_s) \quad (1)$$

where q''_{conv} is convective heat flux, h is convection heat transfer coefficient, T_{∞} is fluid temperature and T_s is surface temperature. The above equation is also known as Newton's law of cooling. Convection can be further divided into natural and forced convection. Natural convection is caused by density changes due to temperature differences, whereas forced circulation is caused by an external driving force such as a pump or reciprocating engine. Quite often in real world situations convection is often mixed comprising from both natural and forced convection. (Bergman et al. 2011, 2–10.)

Thermal radiation is energy emitted by matter at temperatures above absolute zero. The general radiation heat transfer from a surface can be written as

$$q''_{\text{rad}} = \varepsilon\sigma(T_{\text{sur}}^4 - T_s^4) \quad (2)$$

where q''_{rad} is radiation heat transfer, ε is surface emissivity and σ is Stefan-Boltzmann constant and T_{sur} is temperature of the surroundings. (Bergman et al. 2011, 2–10.)

However, in a waste heat recovery application we are interested in the radiation which occur from the exhaust gases to the heating surface. Gases consisting of only so-called nonpolar molecules as O_2 and N_2 can be disregarded as they do not emit nor absorb radiation, but gases containing polar molecules such as CO_2 , H_2O , NH_3 and hydrocarbons emit and absorb radiation in a certain temperature range. With a method created by Hottel the net radiation heat transfer, between the gas and surface can be expressed as

$$q_{\text{net}} = A_s\sigma(\varepsilon_g T_g^4 - \alpha_g T_s^4) \quad (3)$$

where q_{net} is net radiation heat transfer rate, A_s is surface area, ε_g is gas emissivity, T_g is gas temperature and α_g is gas absorptivity. (Bergman et al. 2011, 897–900.) Mäkelä (2019) concluded that the radiation heat transfer from exhaust gases to heat recovery is negligible in temperatures below 600°C.

Conduction is heat transfer across a stationary medium caused by molecular movement. Higher temperature molecules, which have a higher energy content, collide to the molecules of lower temperature and pass a part of their energy to them. The equation for conduction heat flux, called Fourier's law, as follows

$$q''_{cond} = -k\nabla T = -k \left(\mathbf{i} \frac{\partial T}{\partial x} + \mathbf{j} \frac{\partial T}{\partial y} + \mathbf{k} \frac{\partial T}{\partial z} \right) \quad (4)$$

where q''_{cond} is conduction heat flux, k is thermal conductivity and ∇T is three-dimensional temperature gradient. (Bergman et al. 2011, 2; 68–69.)

We can calculate the heat recovered by WHRBs from the exhaust gases with

$$q = \dot{m}_{eg} c_p (T_{eg,in} - T_{eg,out}) - q_{loss} \quad (5)$$

where q WHRB output, \dot{m}_{eg} is exhaust gas mass flow, c_p specific heat capacity at constant pressure, $T_{eg,in}$ is exhaust gas temperature at WHRB inlet, $T_{eg,out}$ is exhaust gas temperature at WHRB outlet and q_{loss} is heat losses from the exhaust gases from the WHRB. The losses are convection and radiation losses from the boiler outer wall to the surroundings. As within the boiler the heat from exhaust gases is transferred by convection to not only the heating surfaces but only to the boiler wall, which the conducts the heat to the outer wall from which heat losses are happen to the surroundings. By combining equation (5) with (1) and (2) we can the output as

$$q = \dot{m}_{eg} c_p (T_{eg,in} - T_{eg,out}) - (q''_{conv} + q''_{rad}) \quad (6)$$

However, when evaluating WHRB heat transfer efficiency we are also interested on what size of a boiler we need. With a composite system consisting of several means of heat transfer it is often best to consider U , overall heat transfer coefficient. The boiler output q can be then stated as

$$q = UAF\Delta T_{lm} \quad (7)$$

where A is overall heat transfer area, F is correction factor for log mean temperature difference for cross flow and ΔT_{lm} is logarithmic mean temperature difference. As we observe exhaust gas flow over tube banks, we use the logarithmic mean temperature difference instead of just simple temperature difference of the fluids, as used in Newton's law of cooling. This is because the temperature of exhaust gas changes while flowing over the tube bank and would otherwise lead to errors in predicting the heat transfer rate. (Bergman et al. 2011, 472). The logarithmic mean temperature difference can be written as

$$\Delta T_{lm} = \frac{(T_s - T_{eg,in}) - (T_s - T_{eg,out})}{\ln\left(\frac{T_s - T_{eg,in}}{T_s - T_{eg,out}}\right)} \quad (8)$$

Overall heat transfer coefficient can be expressed as

$$\frac{1}{UA} = \frac{1}{U_c A_c} = \frac{1}{U_h A_h} = \frac{1}{(hA)_c} + \frac{R''_{f,c}}{A_c} + R_w + \frac{R''_{f,h}}{A_h} + \frac{1}{(hA)_h} \quad (9)$$

where R''_f is fouling resistance, R_w is conduction resistance of tube wall, c denotes cold fluid and h denotes hot fluid.

As seen from Table 1, when we compare the forced convection of gases with the same of liquids or evaporation, the heat transfer coefficient of gases is significantly lower. Hence the highest impact to improve total heat transfer coefficient, which reduces WHRB size, is to enhance the heat transfer of the exhaust gas side.

Table 1. Typical values of the convection heat transfer coefficient (Bergman et al. 2011, 8).

Process	h [W/m ² K]
Free convection	
Gases	2–25
Liquids	50–1000
Forced convection	
Gases	25–250
Liquids	100–20000
Convection with phase change	
Boiling or condensation	2500–100000

To enhance the heat transfer, finned tubes are often used in water tube boilers to increase the heat transfer area. Typical fin types are spiral, gilled and pinned fins. A variety of spiral and gilled fins showed below.



Figure 7. Different spiral and gilled fin tubes (Ekströms Wärmatekniska 2020).

As seen from the above Figure 7, there are several different fin tubes available and basically there are no limits on the geometry. Even though the fin extends the heating surface it does not necessary mean that it would improve the heat transfer compared to a finless tube. The fin is itself a conduction resistance. Selection is done based on exhaust gas characteristics – narrow fin pitches will get clogged more easily, on-line cleanability – tight spacing limits

soot blowing effect on tubes in the middle of the bundle and required heat transfer coefficient – narrow fin pitch together with serrated fins results in the highest heat transfer per meter if tube this reduces the number of tubes and outer dimensions of the boiler. For liquid reciprocating engines gilled tubes are often selected.

The overall surface efficiency η_o of a finned surface can be written as

$$\eta_o = 1 - \frac{A_f}{A} (1 - \eta_f) \quad (10)$$

where A_f is entire fin surface area and η_f is efficiency of a single fin. When consider an extended heating surface on the hot side, we can write the exhaust gas side overall heat transfer coefficient as

$$\frac{1}{U_h} = \left(\frac{1}{h_c} + R''_{f,c} \right) \frac{A_h}{A_c} + R_w A_h + \frac{R''_{f,h}}{\eta_{o,h}} + \frac{1}{\eta_{o,h} h_h} \quad (11)$$

Exhaust gas fouling resistance can be also written similarly as thermal resistance for conduction

$$R''_{f,h} = \frac{L_f}{k_f} \quad (12)$$

where L_f is soot layer thickness and k_f conductivity of the soot layer. It is noteworthy that the soot layer is homogenous in terms of conductivity. (Bergman et al. 2011, 114–116.)

Often instead of fouling resistance, cleanliness factor CF is especially in industrial applications

$$CF = \frac{U_f}{U_c} \quad (13)$$

where U_f is overall heat transfer coefficient of fouled surface and U_c is overall heat transfer coefficient of clean surface (Müller-Steinhagen 2010, 80).

4 FOULING

Fouling can be described as deposition and formation of unwanted substances on any given process surface, in the extent of this thesis on the surface of a waste heat recovery boiler. Fouling is a common problem within heat exchangers where more than 90% suffer from fouling related problems (Müller-Steinhagen 2011, 79). The main reason which make fouling such a large problem is the deposit's generally lower thermal conductivity than steel, usually between 0,2–3 W/mK compared to steel's 36 W/mK. While the deposit thickness increases, in relation the cross-sectional flow path decreases. This leads to high pressure losses over the tube bank. (Awad 2011, 505.)

4.1 History of fouling models

The basis for fouling models was developed by Kern and Seaton (Kern & Seaton 1959). In 1959 they suggested using opposite transport forces, deposit and removal, to model fouling as shown below in Figure 8.

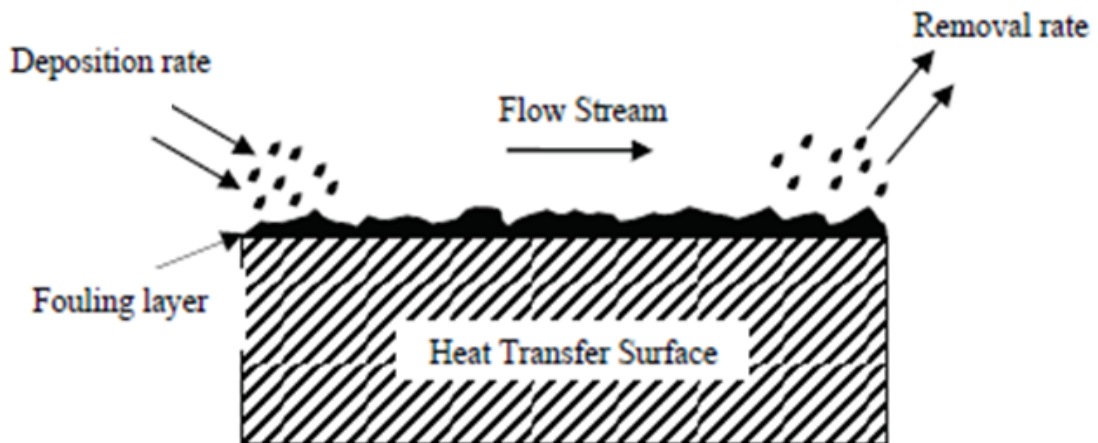


Figure 8. Deposition and removal of soot (Awad 2011, 508).

Developed further in the 1985 by Epstein, where he summarized fouling to follow certain stages described below (Müller-Steinhagen 2011, 4):

- **Initiation**
- **Transport**
- **Attachment**
- **Removal**
- **Aging**

Different fouling resistance with time shown below.

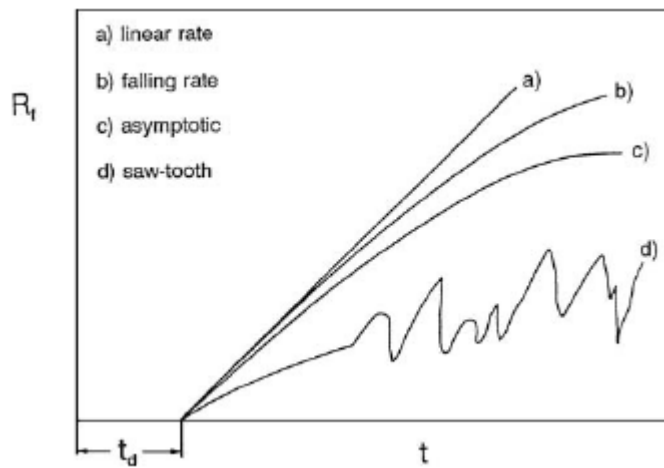


Figure 9. Example of fouling rate with time (Müller-Steinhage 2011, 3).

We can see that the thermal resistance behavior can be different depending on deposit characteristics and application.

For liquid engines typical deposit thermal conductivity is $0,07 \text{ W/m}^2\text{K}$ (Paz et al. 2013, 677).

4.2 Fouling mechanisms

The fouling mechanisms of particles suspended in a flow are presented in the next sub-chapters.

4.2.1 Particle inertial impaction

The tube bundle is an obstacle for exhaust gases and the flow tries to flow around the obstacle. Suspended particles in the flow try to follow the stream around the heating surface, but heavy particles have high inertia which cause them to exit the stream around the bundle and hit the heating surface. This is described as inertial impaction. (García Pérez 2016, 26.)

The tendency for a particle to maintain direct flow path and not avoid the heating surface with the turning flow can be described with Stokes's number. The Stokes's number for a tube obstacle can be written as

$$\text{Stk} = \frac{\rho_p d_p^2 v_p}{9\mu D} \quad (14)$$

where Stk is Stokes number, ρ_p is particle density, d_p particle diameter, v_p is flow velocity upstream from the obstacle, μ is gas dynamic viscosity and D tube diameter.

4.2.2 Thermophoresis

When temperature differences in the flow exist, the gas molecule movement induced collisions on the hot side of the particle are more intense compared to those on the colder side. As heating surface temperature is lower than the surrounding flow the particles are pushed toward the heating surface by thermophoresis. (García Pérez 2016, 28.)

Thermophoresis has been shown to be the dominant deposition mechanism for particle sizes from 0,1–10 μm (Cameron & Goerg-Wood 1999, 51).

4.2.3 Brownian motion

Brownian motion is similar to thermophoresis, but instead of being based more intense molecule impacts on the hot side of the particle like in thermophoresis, the molecular movement and impacts are completely random in Brownian motion. Shortly described as chaotic impacts of gas molecules on the particle, hence the particle motion and direction complete

random as well. Brownian motion only affects small particles, sized similarly as mentioned above for thermophoresis. (García Pérez 2016, 28.)

4.2.4 **Turbulent eddy impaction**

Turbulent flow creates small eddies, which are fluctuations of the velocity components, in the flow. An eddy current directional toward the heating surface can give a particle the required kinetic energy to hit the heating surface. (García Pérez 2016, 28.)

5 CLEANING OF HEATING SURFACES

The heating surfaces of waste heat recovery boilers require cleaning at regular intervals to diminish the effects of fouling, defined in chapter 4 – low performance, pressure losses over the heating surface and keeping flow passages clear which would otherwise eventually result in possible clogging. As engine power plants do not typically include separate soot-collectors (bag filters, electrostatic precipitators or cyclones) other than wet scrubbers Wet scrubbers' main purpose is desulphurization with the capability as a secondary benefit to remove soot from the exhaust gases, but these are always installed after the waste heat recovery boilers. (Läiskä, 2017)

Cleaning methods can be divided into two groups: online and offline cleaning. Online cleaning, from here on referred to as soot blowing, can be carried out during the normal operation of the waste heat recovery boiler, whereas offline cleaning requires stoppage of the heat recovery system. The objective for soot blowing is to maintain acceptable performance and to extend the interval of offline cleaning demand i.e. keeping the fouling layer from reaching or at least slowing down the flow reaching asymptote.

As good praxis the waste heat recovery boilers are designed to comply with a plant specific maintenance interval i.e. in the context of reciprocating engines the running hours of the engine between major overhaul varying between 10000...15000 running hours depending on number of starts and other operation conditions. From a capital investment point of view the use of soot blowers is advised to reduce the initial investment cost, as when using a soot blowing system the excess heating surface required to compensate the effect of fouling is significantly smaller than when not utilizing soot blowing for online cleaning. The risk of soot fire should also be considered if a lot of soot is let to accumulate on the surface, as the soot can include unburnt residues of fuel oil and lube oil.

Within the extent of this thesis the soot blowing focuses on the cleaning of water tube bundles with extended heating surfaces. Different soot blowing methods described below are presented in the following chapters.

- **Steam soot blowing**
- **Air soot blowing**
- **Water soot blowing**
- **Acoustic soot blowing**

Typical offline cleaning methods are water washing, chemical agent washing, dry ice spraying, explosives and different types of mechanical cleaning. These are not investigated further in the extent of this thesis.

5.1 Steam soot blowing

Steam soot blowers are often used as on-line cleaning equipment when the waste heat recovery boiler is generating steam, due to readily available soot blowing medium – steam. The downside of steam soot blowers is that they consume valuable high-pressure steam to cleaning purposes, what could otherwise be used for power generation or alternative applications to generate revenue. Soot blowers are often operated continuously i.e. cycling each soot blower one at a time until the sequence is completed, and the cycle starts again. This leads to a typical steam consumption in soot blowing up to 3–12% of generated high-pressure steam. Industry experience shows, that for liquid engine waste heat recovery boilers the time between sequences can be extended to 3–6 times per 24 hours with an averaged steam consumption of 1–2% of generated steam (Aaltonen 2013, 2). (Pophali et al. 2013, 69).

The basic operation of a steam soot blower is based on high-pressure steam led through a convergent-divergent nozzle (also referred as de Laval nozzle). Commonly used steam pressure ranges between 20–25 bars. Kaliazine et al. (2006) concluded that soot blowing steam pressure can be reduced from 20 bars to 10 bars without significant effect on cleaning performance when mass flow is at the same time increased by 20%. This brings potential savings as high-pressure steam is more valuable than low-pressure steam. The convergent-divergent nozzle accelerates the steam flow downstream of the nozzle to supersonic ($Mach > 1$) velocities, as the nozzles are specifically designed for given steam pressure to create a fully-expanded jet. (Bussman et al. 2013, 5733-5734; Pophali et al. 2013, 69).

Mach number M is a dimensionless number describing the ratio of velocity to sound velocity and can be expressed as

$$M = \frac{v}{a} \quad (15)$$

where M is Mach number, v is flow velocity and a is speed of sound in ambient condition, which vary according to temperature, pressure and medium.

Figure 10. shows basic schematic of a convergent-divergent nozzle.

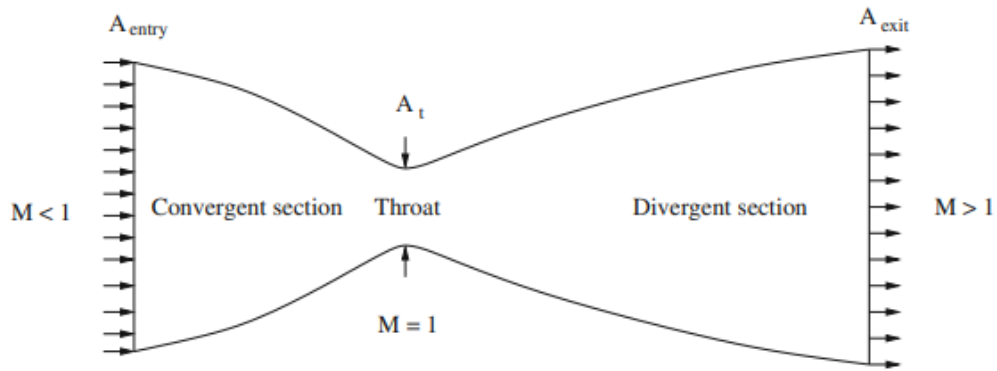


Figure 10. Schematic of a convergent-divergent nozzle (Kaushik 2019, 223).

Fully-expanded jets contain more energy, which results a higher cleaning potential with similar steam consumption compared to over- or under-expanded jets. Under-expanded jets experience shock waves in the nozzle resulting of loss of energy when the steam jet passes through a shock wave. (Jameel et al. 1994, 135)

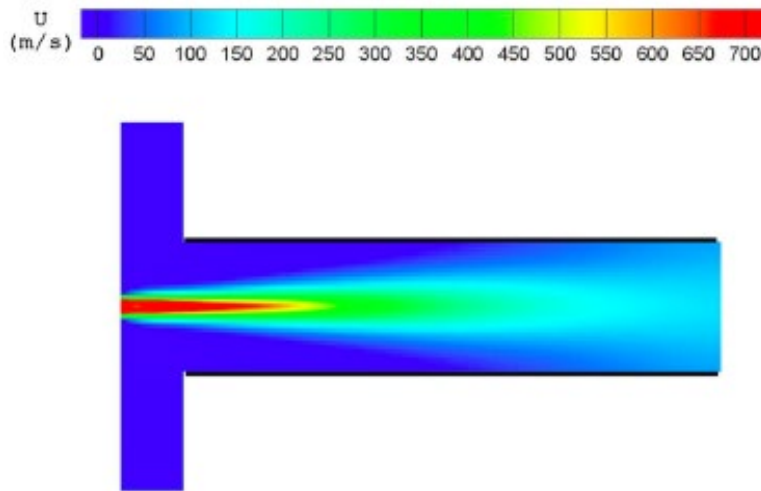


Figure 11. Fully-expanded soot blower steam jet between heating surfaces with an axial velocity. (Bussman et al. 2013, 5734).

As seen from Figure 11 the core of the jet is supersonic. A fully-expanded jet exits the convergent-divergent nozzle at ambient pressure of the boiler. The jet can also be over or under expanded when exit pressure does not match the ambient pressure, which is caused by the supply pressure of steam does not correspond to the designed pressure for the specific nozzle. An over expanded the jet exits the nozzle at a lower pressure than boiler ambient pressure, whereas an under expanded jet exits the nozzle at a higher pressure than boiler ambient pressure. As seen above, the energy of the jet reduces the further it is axially from the nozzle as the velocity jet velocity decreases thus reducing the peak impact pressure (PIP). PIP, dynamic pressure of the jet which can be measured with Pitot-tube) can be used to compare the effect of soot blowing with different nozzles and distances. PIP can be calculated as

$$PIP = \frac{1}{2} \rho v^2 \quad (16)$$

where PIP is the peak impact pressure, ρ is density and v is velocity.

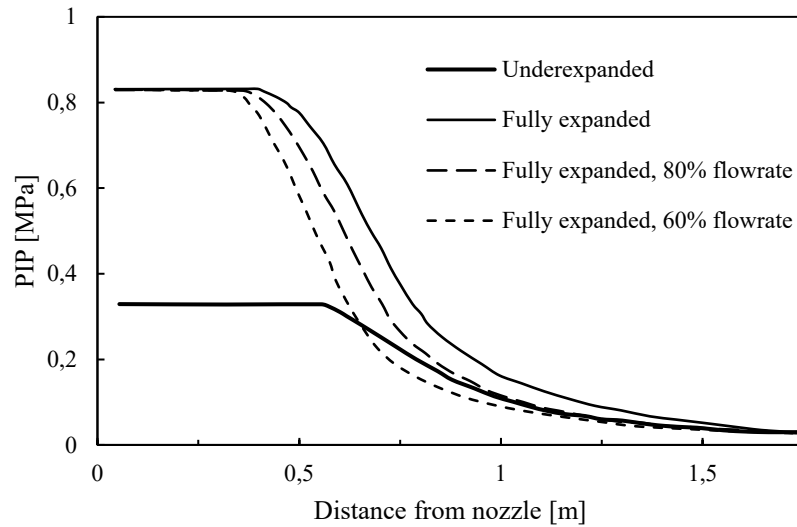


Figure 12. Under and fully expanded nozzles effect on PIP and effective cleaning distance (modified from Kaliazine et al. 1998, 419)

5.1.1 Rake steam soot blower

Rake soot blowers are commonly used to clean tube bundles. The rake construction is illustrated below in Figure 13.

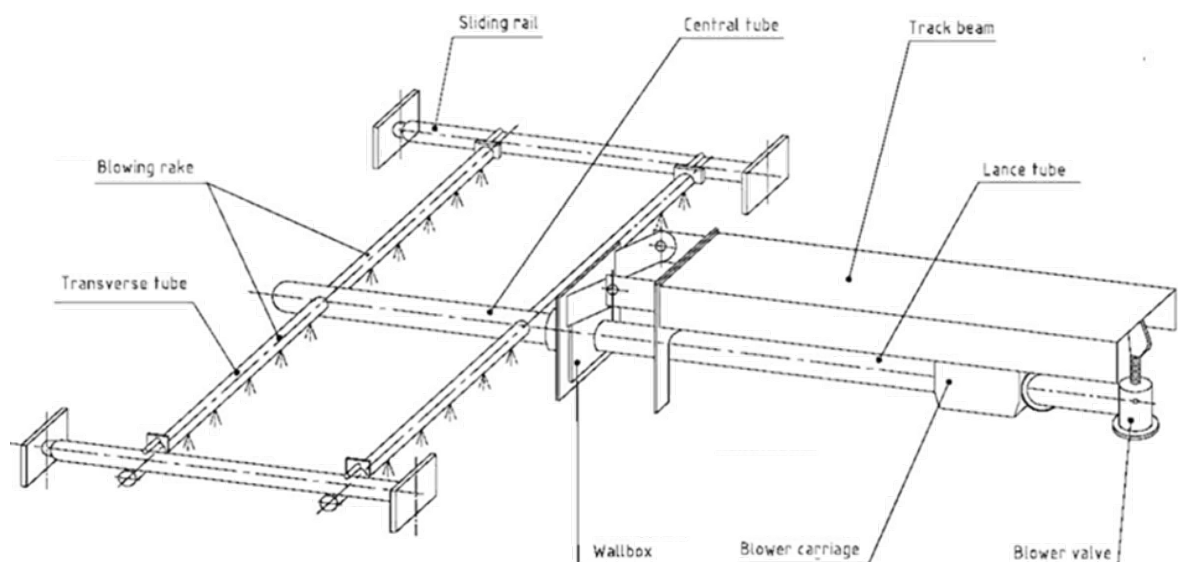


Figure 13. Rake soot blower's basic construction. (Aaltonen 2016; Clyde Bergemann 2020a).

Rake soot blower consists of a central tube, aligned with the stroke direction, that has one or multiple transversal tubes, rakes, on each side. The soot blowing nozzles are evenly situated on the bottom of the rakes. The back-and-forth stroke movement is generated by an electrical motor coupled with rack (track beam) and pinion. A poppet valve is used to adjust steam pressure and flow to the soot blower.

Rake soot blower offers good cleaning effect especially in tube bundles with extended heating surfaces. The cleaning is based on the rake moving laterally above the bundle while soot blowing downwards. The transverse rakes together with the stroke make the rake soot blower cover the complete cross-sectional area of the bundle. Tube bundle with the extended heating surface creates blowing lanes as shown in Figure 14.

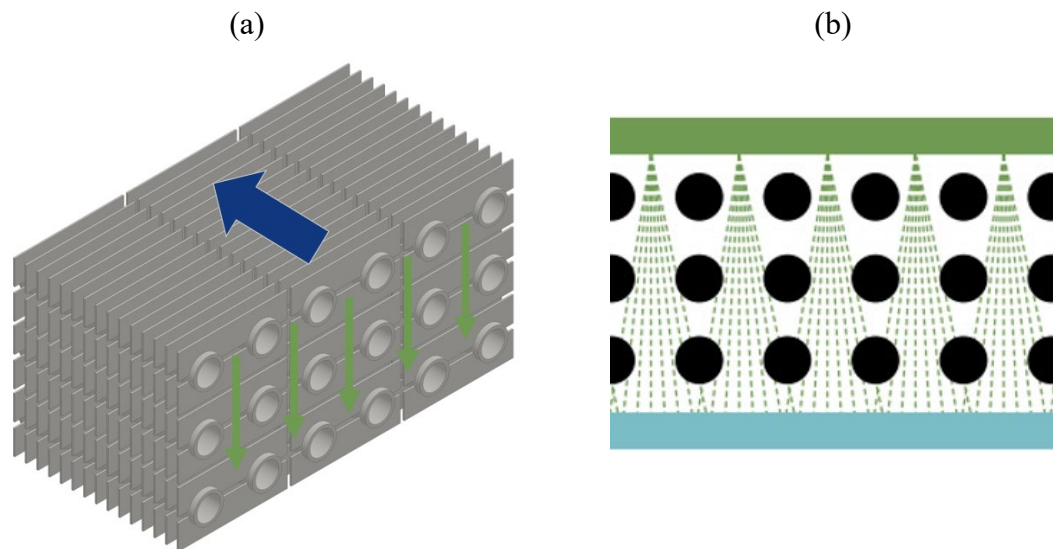


Figure 14. (a) Generic finned tube bundle with blue arrow showing stroke direction and green arrows the blowing lanes on the left (modified from Kakko 2017, 31). (b) General arrangement of a rake type soot blower and blowing lanes (Babcock & Wilcox 2019, 3).

The above Figure 14 shows typical stroke direction and blowing lanes between tubes with inline arrangement in the bundle. Nozzles are relatively small in diameter to create narrow jets to fit into the blowing lanes (Babcock & Wilcox 2019, 3). It is crucial that the spacing of soot blower nozzles is the same as the spacing of blowing lanes for best cleaning results.

In case the tubes were in staggered arrangement the transverse pitch should be greater than tube diameter, for even a narrow blowing lane. To create space for proper blowing lanes by

increasing the transverse pitch of staggered tube arrangement the benefits of using staggered arrangement compared to inline arrangement is lost. Hence inline arrangement is recommended over staggered arrangement for tube bundles with rake-type soot blowers.

5.1.2 Rotating steam soot blower

Rotating soot blowers are inexpensive with a simple and robust construction which is one reason for their popularity. They are fixed to the boiler wall with the soot blower lance penetrating to between tubes or tube bundles. An example of rotation soot blower and basic operation is shown in below.



Figure 15. (a) Rotating soot blower (Clyde Bergemann 2020b). (b) Basic operation principle of a rotating steam soot blower (Clyde Bergemann 2020b).

The construction of a rotating soot blower is for general parts like the rake described in the previous chapter. A lance with longitudinally situated nozzles for the length, electric motor coupled to the lance with a chain drive and a poppet valve. The lance is situated within the boiler between heating surfaces and is rotated by an electric motor around for 360 degrees while soot blowing at the same. Compared to a soot blower with a fixed lance the rotating soot blower reaches a wider area to clean. On the contrary to the rake soot blower with rather small nozzles utilizing lane blowing, the rotating soot blower has larger nozzles. The large nozzles create wider soot blowing cones and have a larger mass flow through an individual nozzle. This type of blowing is often referred to mass blowing, illustrated in Figure 16.

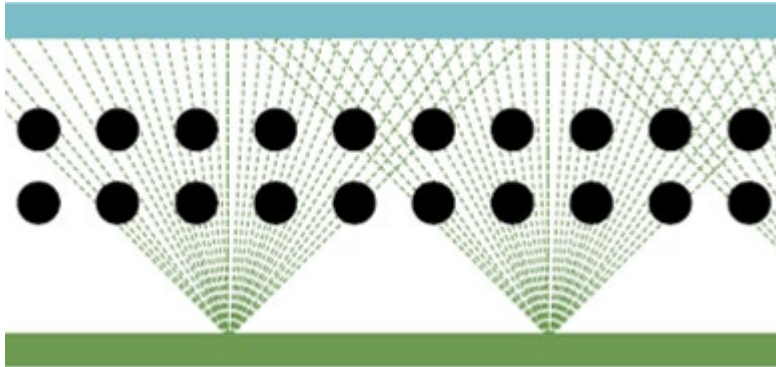


Figure 16. Mass blowing through a tube bundle (Babcock & Wilcox 2019, 3).

Rotating soot blowers are suitable for tube bundles with large cavities, where it can be inserted inside the bundle between tubes and bare tubes in staggered arrangement, where there are no blowing lanes (Babcock & Wilcox 2019, 3). With tube bundles the rotating soot blowers are not as efficient as rake type soot blowers. To cover the entire bundle several soot blowers, need to be situated side by side both above and beneath the bundle. As seen from Figure 16 a wide cone is created which does not have a similar high velocity jet core (Figure 11) as described to be most efficient cleaning in chapter 5.1.

In inline tube arrangements with extended heating surfaces both wide cones and rotating motion hinder the cleaning effect, as the extended surfaces together with inline tubes create narrow blowing lanes. With a wide cone only the middle portion of the steam is blown directly toward the bank, thus that part has a possibility to penetrate deeper to the bank. While the sides of the cone hit the bank diagonally and does not have much cleaning effect on the tubes after the first row of tubes. Similarly, the rotating soot blower have a decent cleaning effect direct above or directly beneath the lance. On tubes further away laterally from the soot blower the soot jet hits the bank diagonally thus the cleaning effect is good on the first row, but narrow lanes created by extended heating surfaces stops the diagonal jet from penetrating deeper into the bank.

5.1.3 Downsides of steam soot blowing - erosion

The engine exhaust gases contain particles as described in chapter 4. These particles get accelerated by the steam soot blowing up to supersonic velocities of the soot blowing jet,

which then increase the erosion caused by particles on tubes. Particle size increase the erosion rate up to sizes between 50–100 μm . After which the increase in particle sizes do not have notable effect on erosion rate. Examples of erosion in tube banks shown in Figure 17 (Wojnar 2013, 473.)



Figure 17. Examples of erosion damage on boiler tubes (Wojnar 2013, 475).

As seen from above Figure 17 the erosion on boiler tubes is a significant problem. The angle of attack influences erosion caused on tubes, for ductile materials the largest wear is between 20–40° from centreline, while for brittle materials the highest is at normal (Wojnar 2013, 473). Wojnar (2013) conducted a study combining CFD and lab tests about the effect of soot blowing on particle erosion. His conclusion was that the largest wear is 40° from centreline as shown below.

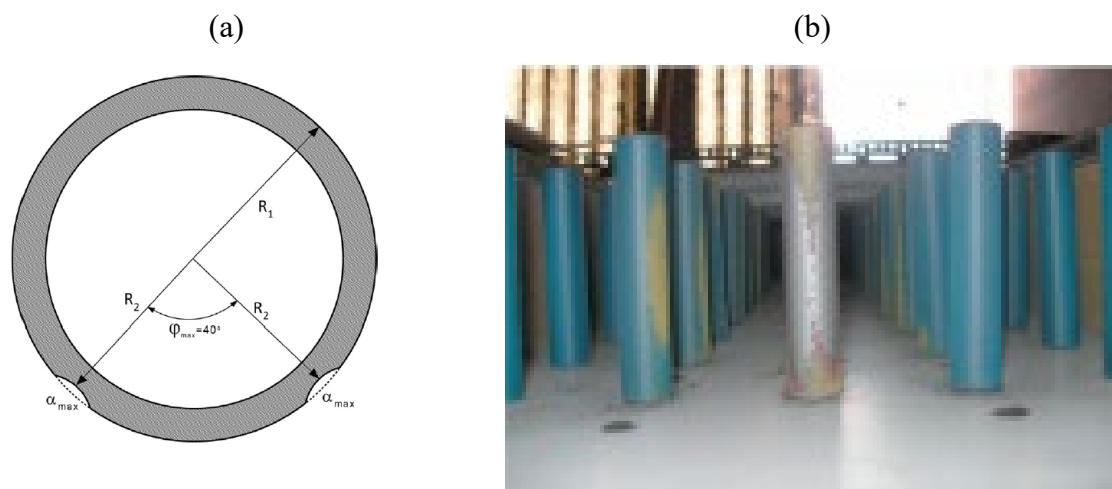


Figure 18. (a) Results by Wojnar showing erosion on tube wall (Wojnar 2013, 476). (b) Test arrangement and visual of test tube bank (Wojnar 2013, 481).

Water droplets accelerated by the supersonic velocities of the soot blower jet can cause similar erosion problems as particles. Water droplets can potentially form after the nozzle due to temperature drop caused by the expansion of steam, but typically the ambient temperature within the boiler is enough to keep the steam superheated within the jet (Wojnar 2013, 488).

However, it is more common that droplets are introduced by improper operation of the soot blowers: **(1) Use of saturated steam**, it is rather difficult to produce saturated steam that is completely dry i.e. wetness fraction is zero, but equally difficult to keep it that way as minor condensation occurs in the piping as the system is not adiabatic. It is highly probable that when saturated steam is used for soot blowing, these condensate droplets are then accelerated with the steam to the tubes. **(2) Condensate in soot blower piping**, after the soot blowing cycle when the soot blower steam valve shuts some of the steam is left in the piping. When the piping then cools down this steam is condensed. Similarly, during soot blower cycle start-up as the piping is at ambient temperature therefore there is condensing of steam happening as the steam valve is opened again to dispense steam to the soot blower. Hence it is important that a proper drain and steam trap system is in place in soot blower piping. Otherwise the remaining condensate would be pushed along the steam to the tube banks in the next cycle. **(3) Soot blowers not pre-heated**, the soot blower itself add to the amount of condensate if it is retractable type as it is kept heat by the hot flue gases within boiler. (Moskal 1996, 91–92.)

5.2 Compressed air soot blowing

Air soot blowers are by construction and operation philosophy quite close to steam soot blowers – only the used medium differs. Most steam soot blowers can be operated with air with just minor changes. There are also multi-media soot blowers available that are designed to be flexible regarding used soot blowing medium.

Compressed air soot blowers use pressurized air between 5–8 bars, with a typical consumption of 450 Ndm³ per signal (Aerovit A/S 2020, 3). As air soot blowing does not consume steam it is an alternative for plants operating on hot water or other media, like thermal oil. The downside with pressurized air soot blowers is the relatively high electricity consumption of the compressors required to produce the pressurized air as the soot blowers have to be cycled continuously (Luoti 2020). Aerovit's patented air soot blower system is shown in Figure 19.

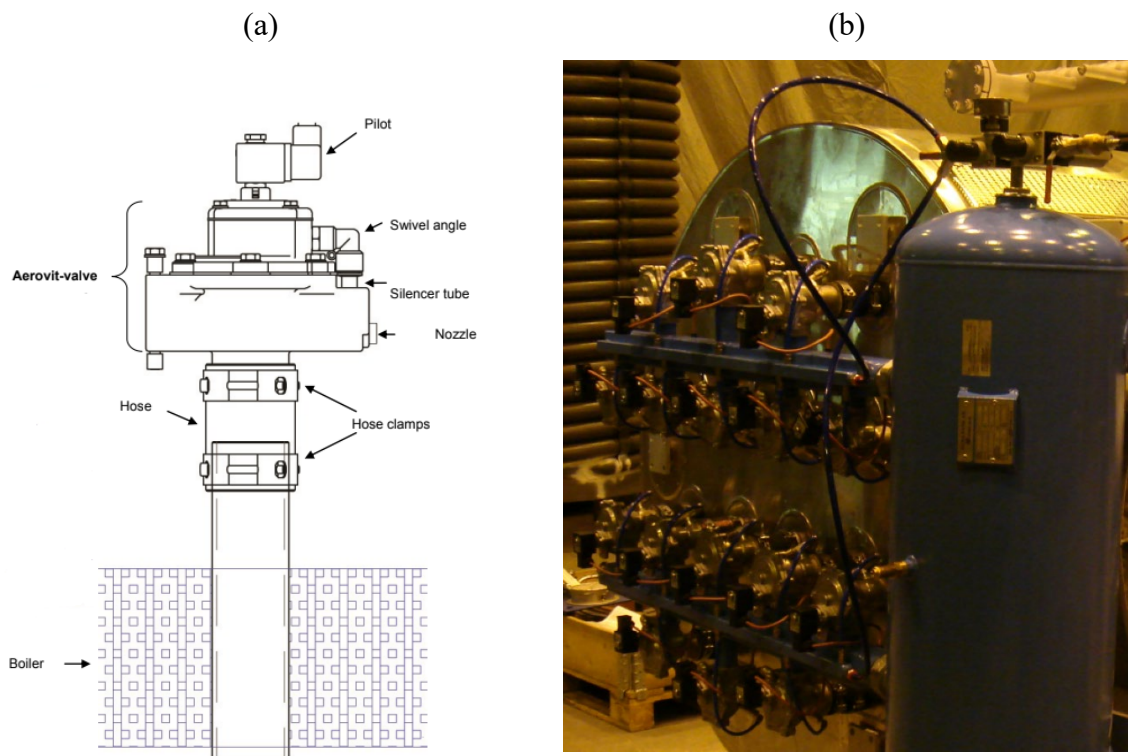


Figure 19. (a) Aerovit's air soot blower (modified from Aerovit 2020, 5). (b) Aerovit air soot blower system installed to a smoke tube boiler (Alfa Laval Aalborg Oy 2009).

Typically, air soot blowers as shown above Figure 19 are only used for smoke tube boilers. For cleaning of tube bundles the air soot blowers are similar rake- or rotating-type soot blowers used for steam as described in chapters 5.1.1 and 5.1.2. Tube erosion is also possible due to particles being suspended into the air jet and hitting tube wall at high velocities, similarly as with steam.

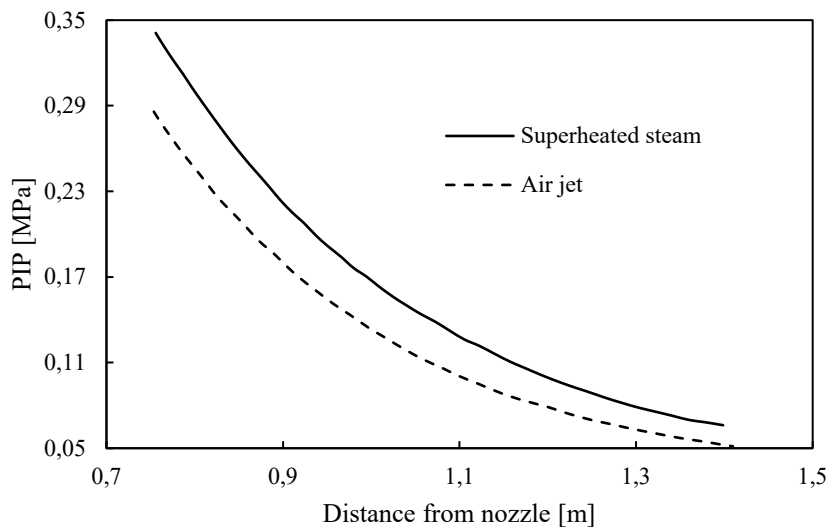


Figure 20. PIP for superheated steam and air as distance from nozzle, pressure for both is same (modified from Jameel et al. 1994, 141).

As seen above compared to steam soot blowers the air has lower PIP with same pressure, while air consumes twice the mass flow compared to steam when used with the same nozzle.

5.3 Water soot blowing

Water soot blower can be used basically with the same construction or with very small changes of the one of steam soot blower. Water soot blower offers great cleaning effect as water has higher density than steam or air. The downside is high erosion caused by droplets and thermal shocks when the water hits the heating surface.

5.4 Acoustic soot blowing

Acoustic soot blowers, also referred to as acoustic horns, are soot blowers utilizing sound waves to clean the heating surfaces. Sound waves can be divided by frequency according to

the human hearing range to infrasound <20 Hz, audible sound 20–20000 Hz and ultrasound >20000 Hz, of which infrasound waves are commonly used for boiler cleaning due to their best cleaning effect of the three. Large flat surfaces, like ducting, are susceptible for infrasound induced vibrations, hence low, audible frequencies <200 Hz are sometimes used as well to avoid structural damage to the boilers. The objective is to avoid the natural frequency of the surrounding system, at which it oscillates naturally without acoustic soot blower sound waves. If the sound waves' frequency matches the natural frequency of the system by some multitude the system starts resonating, which may cause damage to the structure. Typically used acoustic soot blowers produce sound pressures between 135–175 dB for efficient cleaning result. (Schimmoller 1999, 20.)

The acoustic soot blowers use pressurized air between 5–8 bar to create sound waves. Typical air consumption during the 5–10 second cycle ranges between 20–400 Ndm³/s depending on size and whether it is audible or infrasound type. Usually the plant's instrument air system can be used for pressurized air supply, but with soot blowers with higher consumption additional compressors and air receiver tanks might have to be considered. An example construction of an acoustic soot blower utilizing infrasound waves is shown in Figure 21.

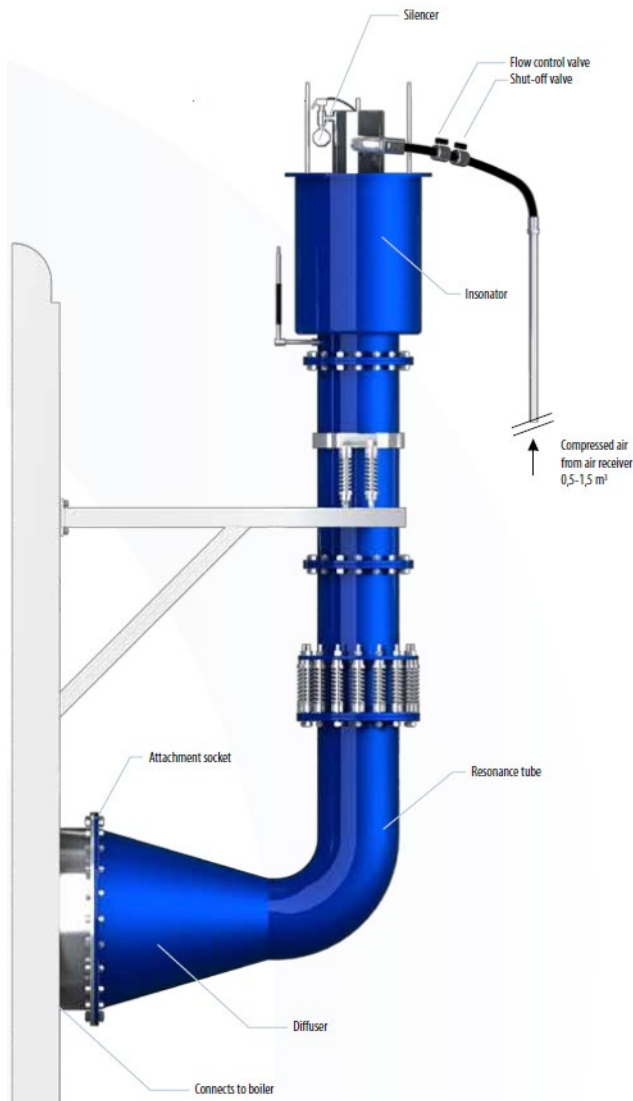


Figure 21. Acoustic soot blower assembly using infrasound waves (Heat Management 2020).

In the above figure there are three main parts in acoustic soot blower: insonator/ oscillator, where the pressurized air is transformed into infrasound waves, resonator tube, where the sound waves are resonated and diffuser/ horn, which amplifies the sound waves into the boiler. Horn type acoustic soot blower, which are typically used with audible frequencies shown below in Figure 22.



Figure 22. Acoustic horn (Kockum Sonics).

There are two phenomena that acoustic soot blowers utilize for cleaning: (1) vibration and (2) collapsing of the boundary layer on heat transfer surface. Infrasound waves created by the horns cause the particles suspended in the flue gas and in the soot layer to oscillate. The oscillating particles' energy is higher than the adhesive forces that keep the soot layer intact to the heating surface. The soot layer break and the particles are swept away with the flue gas stream as shown in Figure 23. The oscillation also breaks soot clumps into separate particles and stops particle attachment on the surface, hence acoustic soot blowers are typically used as preventive means of cleaning. The cleaning effect is significantly lowered if the particles in the soot layer have had time to sinter together to form a hard soot layer. (Kockum Sonics 2008, 3; Borovikov et al. 2005, 477.)

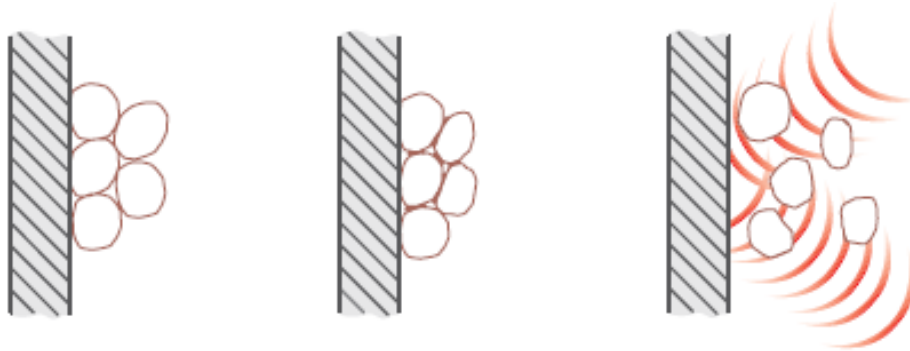


Figure 23. Infrasound waves hitting heat transfer surface covered with soot particles (Kockum Sonics 2008, 3).

The high sound pressure level sound waves have higher energy content than the flue gas without sound waves. The sound waves increase turbulence of the flow and collapse the boundary layer on the heating surface essentially increasing surface flow velocity as shown below in Figure 24.

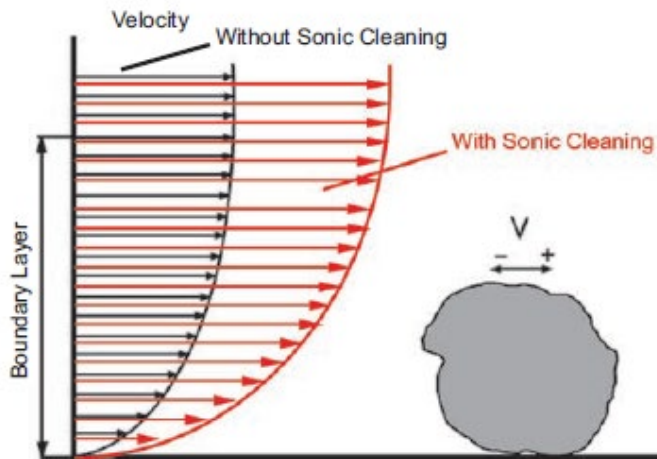


Figure 24. Effect of acoustic soot blowing on boundary layer characteristics (Kockum Sonics 2008, 3).

Schimmoller (1999) have summarized the required conditions for efficient acoustic soot blowing as follows:

- Low moisture content – Acoustic cleaning works best on dry and powdery deposits with recommended moisture content less than 15–20%.
- Sound pressure level – Needs to be high enough (>135 dB), not just at horn outlet, but throughout the boiler to ensure proper cleaning result.
- Time between cycles – Needs to be short enough so particles do not have time to sinter together which raises their adhesive forces, typically 5–15 minutes interval

between cycles is used with cycle length of 5–15 seconds. The interval depends on fouling characteristics of the flue gases.

- Particle removal – Sufficient flue gas flow velocity (>5 m/s) need to be introduced across the heating surfaces to remove particles swept loose by the acoustic soot blowers. For vertical flows gravity helps in removing the loosened soot particles, hence sufficient flow velocity is not as important.
- Surface cleanliness: Best overall effect of acoustic cleaning is achieved when it is done rather pre-emptive before soot layer has accumulated than when noticeable drop in performance has already occurred.

Compared to steam soot blowing acoustic soot blowing offer low O&M costs as it does not consume valuable steam, nor does it have many moving parts which require maintenance or are susceptible for wear-and-tear. Acoustic soot blower is gentle to heating surface as only the sound waves are hitting the heating surface so there is no mechanical wear or erosion. Also, no additional medium is introduced to the flow that might cause corrosion when reacting with the soot layer. Acoustic soot blower can potentially save space compared to steam soot blowers which require cavities or cleaning spaces between tubes or tube bundles, when acoustic soot blower is more flexible regarding with its siting as sound waves does not lose energy as quickly as a steam jet. Acoustic soot blowers can clean the backside of the tubes, staggered arrangements, and other complicated geometries, due to the nature of sound waves reflecting from surfaces. However, special attention must be put on the design and dimensioning of the acoustic soot blower for sufficient cleaning throughout the boiler. The major downturn is that the cleaning effect is not enough cleaning sticky, wet or hard soot layers or when the soot layer has had time to build-up. Schimmoller (1999) sums it up “Sonic cleaning devices are designed for keeping a surface clean, not getting it clean”. (Schimmoller 1999, 19–26.)

Developed in the 70s, the popularity of acoustic soot blowers has taken some falls in the past due to failed dimensioning, and together with general disbelief of operators that sound waves could do proper cleaning they have stayed as a quite niche product. Similar experiences have also been observed at Alfa Laval Aalborg oy, with acoustic soot blowers either working fine or not working at all (Aaltonen, 2017). This has been due to errors in designing the acoustic soot blowers and overlooking soot characteristics. With today’s better understanding and know-how on acoustics there could be place for these to slow down the deposition on heating surfaces.

6 CASE STORY: ECC PLANT IN SOUTH ASIA

This chapter describes shortly the power plant and, in more detail, the WHRB system. The measurements were conducted during a site audit in 2017.

The ECC plant was commissioned in 2016. It has three MAN 18V48/60TS 18 MW_e diesel engines operating on HFO with their corresponding auxiliary system and a steam system running a 2,35 MW_e STG. At design point the exhaust gas flow for each individual engine is 34,24 kg/s and 338°C. The exhaust gases of each engine are led to individual WHRBs where heat from the exhaust gases are recovered to produce superheated steam at 16,1 bar(a) @ 270°C. The steam from each WHRB is collected to a steam header from which it is led to the STG.

The investigated WHRB is a vertical water tube type boiler with extended H-type finned heating surfaces, comprising of a HP superheater, HP evaporator, HP economizer and LP evaporator sections. Tubes are arranged into inline bundles. Each WHRB is equipped with two rake soot blowers, similar as described in 5.1.1, which use superheated steam as blowing medium. This reduces the amount of steam available for the STG during soot blowing cycles. Due to relative low exhaust gas temperature having a low pressure section, that would generate steam at sufficient pressure and superheat (as we concluded in chapter 5 requirement is superheated steam at a minimum pressure of 10 bars) to be used for soot blowers was deemed too expensive during sales phase of this project.

Per discussions with the Plant Manager their typical interval between water washing has been every 2–3 months. With one WHRB blind flanged and bypassed so that the engine can run normally during water washing, while the two others WHRBs continue to produce steam for the STG. Typically soot blowing cycles are conducted 3–4 times a day when the outlet temperature reaches its set value. Typical weekly operation hours are from 9:00–18:00 six days a week. This corresponds to about 300 engine starts into the WHRB in a year, when water washing outages and a yearly engine overhaul is considered. The actual number of starts is probably something between 300–500 starts a year due to unscheduled downtimes, as during the two days on there was a total of 3 emergency shutdowns of engines due to electrical grid instability.

7 RESEARCH METHODS

In this part the long-term reduction in performance due to fouling of heating surfaces in the ECC power plant, described in the previous chapter, is studied. The effect of soot blowing to prolong manual water washing interval and sustain adequate steam generation performance is also studied. The objective was to receive more information of the effect of fouling and soot blowing on WHRB performance. This would be later used to optimize fouling margin calculations for future cases and to give certainty for performance guarantees. Suggestions of optimal soot blowing and water washing interval, and improvements that reduce steam consumption was also a target.

7.1 Measurements

The intended measurements can be divided into two groups – measurements done on site and data analysis of collected data from plant's logged control system data.

Measured values / intended measurement points are:

- WHRB steam flow before and after soot blowing
- Measurements of soot layer thickness and visual inspection

Data to be collected from plats:

- Turbine output [MWe]
- Superheated steam flow in main steam line [kg/s]
- Superheated steam pressure in main steam line [bar(a)]
- Superheated steam temperature in main steam line [°C]
- Exhaust gas side inlet / outlet temperatures [°C]
- Feed water tank temperature [°C]
- Steam drum pressure [bar(a)]
- Engine load [%]

Additionally, to get a better view of long-term fouling the dates of water washes were to be asked from the site personnel.

7.1.1 WHRB steam flow before and after soot blowing

As there were no individual steam flow meters for WHRBs, a non-intrusive ultrasonic clamp-on flow meter was used. Used flow meter was Flexim Fluxus F601, which is suitable

for measuring flow velocity of liquids with volumetric and mass flow calculated with input parameters of the liquid and pipe size. The measuring accuracy of the flow meter is $\pm 1,6\%$ and last calibration done in 2015, the calibration is good for 36 months. Measurements were conducted both before and after soot blowing to evaluate the effect and to make comparisons to data analysis from plant's logged control system data.

According to mass balance the mass flow of the feed water flow entering and the mass flow of superheated steam leaving boundary limit are equal when there are no other inlets or outlets.

Other actions that were done prior to start of the measurements were:

1. WHRB bypass damper was driven manually to be fully open – this was to ensure the sealing tightness toward bypass duct.
2. Manual throttle valve was adjusted to keep feed water flow steady and automatic feed water valve was bypassed. The feed water valve will control feed water flow to drum water level close to normal water level (NWL). This was also inspected prior and after the measurement that the level was kept at or close to NWL.
3. Bottom blow down and surface blow out from steam drum were closed for the measurement period.
4. Engine load was locked on 100%.
5. Turbine load was adjusted so that the steam drum pressure would stay as stable as possible.
6. Feed water tank temperature were to be kept as stable as possible.

The location for transducers, which are the measuring heads, was selected according to the user manual of the Flexim Fluxus F601. Most importantly that there was sufficient distance after or before any flow disturbance source such as elbows, valves, pumps, reducers and diffusers. Typical distances according to the manual are 10–50 D, where D is pipe diameter, after disturbance source and 5–10 D Secondly the measurement location had to be a horizontal pipe or vertical pipe. Requirement for horizontal was to have transducers clamped on the side, for vertical transducers the water flow direction should be upwards. Lastly the general geometries of the piping should be so that the measurement point is not in a “dip”, which could lead to the pipe not being full of water. (Flexim 2010, 17–20.)



Figure 25. Fluxus measurement head clamped to feed water piping which have its insulation removed from measured section, with direction of water flow being toward the photographer.

Recommended distance from the pipe elbows in this situation would have been $40 D$, which this do not quite fulfil as seen from above Figure 25. This was however found to be the best location in terms of accessibility to conduct measurements and site personnel to remove the insulation and cladding and clean the pipe surface from any deposits.

The flow meter was set to show mass flow and calculate cumulative flow over a period of 1 hour to reduce the effect of flow fluctuations in the results.

7.1.2 Soot layer thickness measurement and visual inspection

Soot layer thickness measurements and visual inspection of the inside was conducted on WHRB no. 2, by construction it is similar as no. 3 for which flow measurement were done. The corresponding engine was under maintenance so the insides of boiler no. 2 could be accessed. Doing both internal inspection and flow measurements on the same boiler would have taken too long as the boiler take at least 1 day to cooldown after the engine is shut down

and timing with engine maintenance would have been more difficult as well. The soot layer thickness was measured with a wet film thickness gauge and a vernier caliper with a depth measuring blade. The thickness gauge was used to measure thin layers less than 0,5 mm thick, and the vernier caliper for thicker deposits.

As the WHRB has two tube bundles the thickness was measured from each both from above and below. The tools did not fit between tube rows or columns due to boiler and tube bundle structure, hence only the outmost tube row on the top and bottom of the banks could be measured. Similarly, due to fins only the flat wide part of the fin could be measured close to the open area.

8 RESULTS

In this part the measurements and data analysis are presented. First part consists of effect of soot blowing on WHRB output which were measured with ultrasonic flow meter. Second part consists of visual inspection of heating surface and soot layer thickness measurements. Lastly the results of decrease of boiler performance are presented based on data analysis done on plant's logged control system data.

8.1 Effect of soot blowing on WHRB output

Flow measurements were conducted for EGB no. 3 on 13 May 2017. The WHRB had been water washed on 21st April 2017 i.e. 22 days prior to the measurements. As concluded in average exhaust gas inlet temperature, steam drum pressure and superheated steam temperature has been calculated over the measurement time span of 1 hour for each measurement. As there are small differences in the pressure and temperature of steam, recovered heat is calculated.

Table 2. Steam flow measurements before and after soot blowing.

Measurement	\dot{m}_s [kg/h]	$T_{eg,in}$ [°C]	T_{fw} [°C]	p_{sup} [bar(a)]	T_{sup} [°C]	q [kW]
Before soot blowing	5742	329	130	14,3	272,3	3878
After soot blowing	5964	330	133	15,2	274,4	4010

Heat transfer rate can be calculated from the measurements with the following equation

$$q = \dot{m}_s (h_{sup} - h_{fw}) \quad (17)$$

where \dot{m}_s is steam mass flow, h_{sup} is enthalpy of superheated steam and h_{fw} is enthalpy of feed water. Engine exhaust gas values were assumed to be the same for both measurements. The result could be verified by calculating the heat rate recovered from exhaust gases with equation (6).

However, there are too much uncertainty about the engine mass flow if site rated condition is used. Typically, the mass flow can fluctuate ± 5 –10% from rated flow depending on e.g.

ambient temperature, condition of the engine and temperature of the cooling circuits. The mass flow could be determined by calculating it from engine fuel flow, O₂-content in exhaust gases, fuel analysis of used fuel and engine power, but even calculated like this the uncertainty is estimated to be $\pm 8\%$ (Pöyry 2013, 1–2).

8.2 Soot layer thickness measurements and visual observations

The soot layer was measured from four different locations of WHRB no. 2 shown in Figure 26. Soot blowing sequence had been done 15 minutes before shutting down the engine. The personnel did not have knowledge of the last water wash.

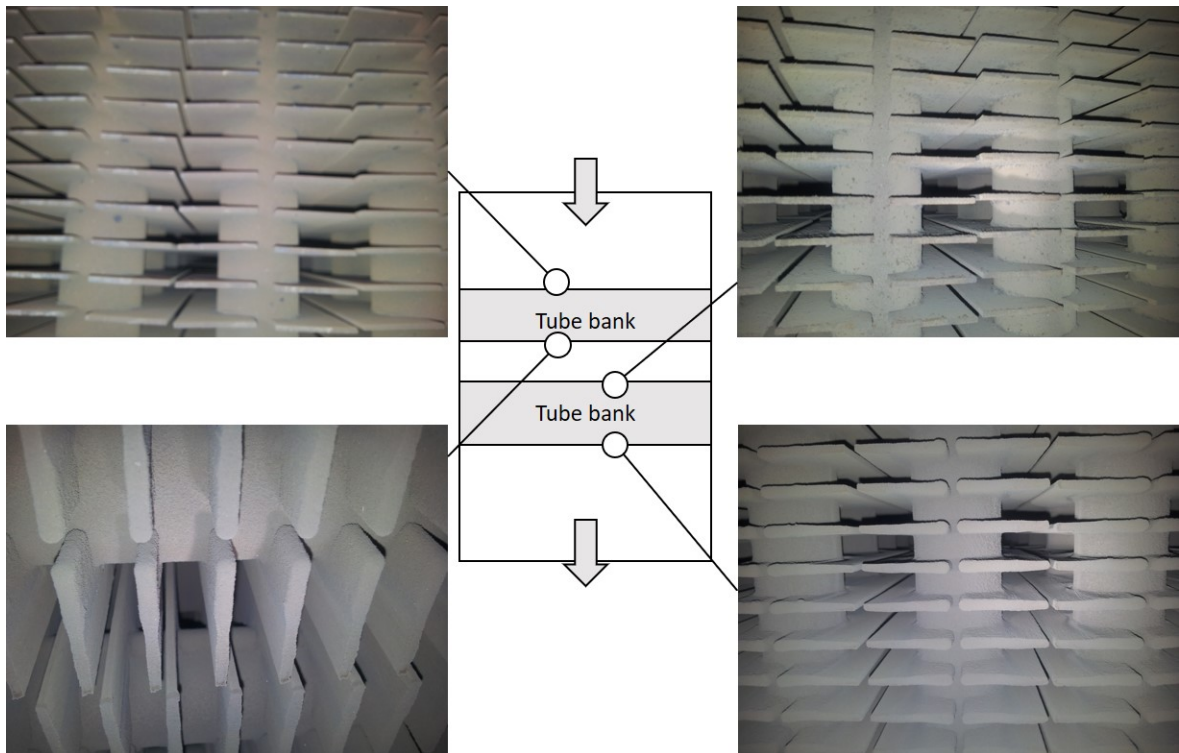


Figure 26. Photos of heating surfaces from different locations showing thickness measurement places.

Measurement places and taken photos can be seen from the above figure. Top part of both bundles looks to be relatively clean, clearly due to the soot blowing cycle done prior to shut down. From below visually the soot layer is clearly thicker directly under the tubes and thinner closer to the edges. There is no sign of any incipient clogging. Soot blowing lanes, which were shown in Figure 14 and discussed in 5.1.1, can be clearly seen between tubes and fins.

Soot layer thickness measurement shown below Table 3. It was quite impossible to get accurate results with the measurement as the soot was dry and powdery, and it did quite easily just fall off when trying to measure its thickness from fin surface. Fouling resistance can be calculated with equation (12) and thermal conductivity for deposits after diesel engines 0,07 W/mK.

Table 3. Soot layers thicknesses measured from different locations and calculated fouling resistance.

Measurement point	L_f [mm]	R''_f [m ² K/W]
Upper register top	0,1	0,00143
Upper register bottom	0,2–1,5	0,00286–0,0214
Lower register top	0,1	0,00143
Lower register bottom	0,2–1,5	0,00286–0,0214

8.3 Data analysis from control system's logged data

From the plant's operating system only about a month's backlog was stored, so no long-term fouling curve is available. For simplest presentation a curve of exhaust gas outlet temperature with running hours with the bypass damper fully open into the boiler was made.

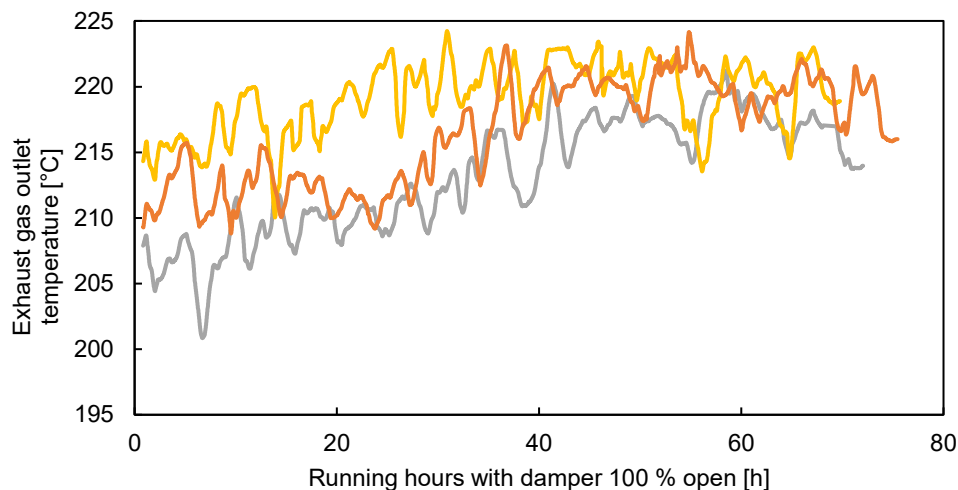


Figure 27. All boilers running in the end of April 2017.

The design outlet temperature for the boiler is 200°C.

9 DISCUSSION

9.1 Soot layer thickness measurements and visual inspection

As seen from Table 3 and based on visual inspection done on the insides of the WHRBs the soot layer thickness varies a lot. Not only within the bundle but also within a single fin and respective tube portion to which the fin is welded. That added with fact discussed in Chapter 4 of the soot layer is not uniform throughout its thickness. The soot layer tends to be more packed and dense close to heating surface and more porous and loose close to the flow regime. Equation (12) was used to determine the fouling resistance, using homogenous conductivity assumption. As the soot layer thickness varies a lot, the total fouling resistance cannot be determined precisely, only the range of variation could be solved.

It can be concluded that measuring the soot layer thickness is not a viable way to determine fouling resistance over the entire boiler. It is also rather troublesome to conduct the measurements as the waste heat recovery boiler needs to be taken out of service and let it cool down for a day. However, if we would use CFD to model the fouling of heating surfaces the visual inspection and thickness measurement would be imperative to validate the model empirically.

A general value found from literature for the thermal conductivity of the soot layer was used. A soot sample could have been taken and analyzed in a laboratory for more accurate results, as the fuels the engine burns do vary by composition and additives. This is recommended to be done for future cases.

No difference in deposition between the upper tube bank being in the hotter and the lower tube bank being in the colder end of the WHRB can be seen.

From the visual inspection and thickness measurements we can conclude that the soot blower is working as it is supposed. Soot blowing lanes, as illustrated in Figure 14, can be clearly seen from the photos taken from site in Figure 26. As expected, the fin area on the sides (not

shadowed by the tube) has a thin soot layer owing to effective lane soot blowing and correctly sized cross-section for high enough flow velocities. When insufficient cleaning is present the heating surface can start to clog as shown below.



Figure 28. An almost clogged tube bundle in a WHRB after a reciprocating engine burning LBF. The WHRB was running for an extended period with a broken rake soot blower which was left unnoticed.

Above a clogged heating surface can be observed. The soot layer thickness and thus fouling resistance increases so much that the medium within the tubes is not cooling the hot exhaust gases. This leads to high temperature on the exhaust gas side surface of the deposit which ultimately could lead into a soot fire as the soot after engines contain some amounts of unburnt particles.

9.2 Long-term performance based on plant's logged control system data

Figure 27 presents the development of outlet temperature over time. While the initial outlet temperature for a clean boiler have been 200°C, but as the exact mass exhaust mass flow is not known the temperature curve works more relatively rather than they could considered as absolute values. We can see that after 40 hours the boilers reach their asymptote where the WHRB is not reducing anymore, which means that removal and deposition of the soot layer

is equal. Small spikes are caused by the soot blower when the performance is higher for a short while resulting in a lower outlet temperature.

As site measurements in a large scale are rather difficult to conduct especially if a longer period should be observed. For better results remote connection and enough measuring points should be utilized to transport the data directly from site's control system to office for big data processing. This would not only provide easy on-line evaluation of performance and effect of cleaning for a single boiler but could be easily scaled for multiple boilers and multiple plants from around the world. Recommended instruments for optimal measurements given in Table 4.

Table 4. Recommended instruments for remote monitoring.

Instrument		
Temperature transmitter, WHRB inlet	T	°C
Temperature transmitter, WHRB outlet	T	°C
Pressure difference measurement over boiler heating surface	Δp	Pa
O ₂ -analyzer to exhaust gas duct	O ₂	v-%
Engine fuel flow (from engine control system)	\dot{m}	kg/s
Engine power (from engine control system)	P_e	MW _e
Fuel analysis (from engine control system/when available)	-	v-%

The above would be the minimum to determine heat recovered from the exhaust gases and to evaluate long-term reduction in performance precisely. Additionally, all typical operating values would be available as well so any problems with plant operation could be pointed out.

9.3 Soot blowers

As Figure 26 and Table 2 showed excellent soot blowing effect even on the bottom part of the tube bundles as well. In order to reduce steam consumption the soot blower control could be modified so that the steam is only dispensed during the return stroke. This would at the same time also allow the hot exhaust gases to preheat the central tube before steam is introduced to reduce condensation and possible water droplets in steam jet. Further to reduce

steam consumption an acoustic soot blower could be installed to one boiler to test if the soot blowing period could be prolonged.

10 CONCLUSIONS

Fouling relies still a lot on empiric tests and industry experience. While numerical models are more and more emerging to predict more accurately fouling. The results need to be often verified in a test bench or at site. As fouling as a phenomenon and different soot characteristics vary a lot, not only between processes, but also within the same boiler during the day.

Regarding on-line cleaning methods in general and the soot blower-deposit interaction not much development has been done during this millennium. Most of the on-going research and development seems to be done within companies providing different cleaning systems.

Usually there are multiple engines on plant which brings the opportunity to compare two different on-line cleaning methods rather easily as the boilers are often identical and with 1:1 coupling. Of course, there is slight variance in engine operation (even though they are identical) due to different wear on parts, running mode (starts and load).

As site measurements in a large scale are rather difficult to conduct especially if a longer period should be observed. For better results remote connection and enough measuring points should be utilized to transport the data directly from site PLC to office for big data processing. This would not only provide easy on-line evaluation of performance and effect of cleaning for a single boiler but could be easily scaled for multiple boilers and multiple plants from around the world.

The following recommendations were concluded to save steam in case story plant: Steam to dispensed only during soot blower return stroke and acoustic soot blower to be installed to prolong soot blowing interval.

REFERENCES

Aaltonen, P. 2009. WHR BASIC DESIGN – Sootblowing of exhaust gas boilers. Alfa Laval Aalborg Oy intranet: Access rights needed. (accessed 15 January 2020).

Aaltonen, P. 2016. Fouling & cleaning of boilers. Alfa Laval Aalborg Oy intranet: Access rights needed. (accessed 15 November 2020).

Aaltonen, P. 2017. Technology Manager, Alfa Laval Aalborg Oy. Rauma. Interview October 2017.

Aerovit A/S. 2020. Aerovit – Data and operating instructions for running and maintenance of soot removal system. [brochure]. Available online: <https://www.aerovit.dk/products/manual.php> (retrieved 16 November).

Adefarati, T., Papy, N.B., Thopil, M. & Tazvinga, H. 2017. Non-renewable Distributed Generation Technologies: A Review. In Handbook of Distributed Generation: Electric Power Technologies, Economics and Environmental Impacts. Bansal, R. (ed.). 2017. p. 69–105. Cham: Springer International Publishing AG. ISBN 978-3-319-51343-0.

Alfa Laval Aalborg Oy. 2009. [photograph]. Alfa Laval Aalborg Oy intranet: Access rights needed. (accessed 15 November 2020).

Alfa Laval Aalborg Oy. 2020. AV-6N waste heat recovery boiler.

Babcock & Wilcox. 2017. Diamond Power G9B. [brochure]. Available online: <https://www.babcock.com/en/products/sootblowers/-/media/b3016250d151454982d4c3c3a91deefc.ashx> (retrieved 15 November 2020).

Bergman, T. L., Lavine, A. S., Incropera, F. P. & Dewitt, D. P. 2011. Fundamentals of Heat and Mass Transfer. 7th edition. John Wiley & Son, Inc. 1048 p. ISBN 978-0470-50197-9.

Borovikov, V., Kleesmaa, J. & Tiikma, T. 2005. Analysis of Experimental Results of Sonic Cleaning System in Oil Shale Boiler. *Oil shale*, vol. 22: 4 Special, p. 475–485. ISSN 0208-189X.

Breeze, P. 2019. *Power Generation Technologies*. 3rd edition. Elsevier. 978-0-1281-8255-0. Retrieved from: <https://app.knovel.com/hotlink/toc/id:kpPGTE001C/power-generation-technologies/power-generation-technologies>.

Bussman, M., Emami, B. Tandra, D., Lee, W. Y., Pophali, A. & Tran, H. 2013. Modeling of Sootblower Jets and the Impact on Deposit Removal in Industrial Boilers. *Energy & fuels*, vol. 27, p. 5733–5737.

Cameron, J. H. & Goerg-Wood, K. 1999. Role of thermophoresis in the deposition of fume particles resulting from the combustion of high inorganic containing fuels with reference to kraft black liquor. *Fuel processing technology*, 60, p. 49–68.

Clyde Bergemann. 2020a. Clyde Bergemann Power Group [www-page]. Available online: <https://www.cbpg.com/en-gb/products-solutions/boiler-efficiency/load-boiler-cleaning-systems/economiser/rake-sootblower> (accessed 3 November 2020).

Clyde Bergemann. 2020b. Clyde Bergemann Power Group [www-page]. Available online: <https://www.cbpg.com/en-gb/products-solutions/boiler-efficiency/load-boiler-cleaning-systems/economiser/rotating-element-sootblower> (accessed 3 November 2020).

Clyde Bergemann. 2020c. Clyde Bergemann Power Group [www-page]. Available online: <https://www.cbpg.com/en-gb/products-solutions/boiler-efficiency/load-boiler-cleaning-systems/economiser/oscillating-sootblower> (accessed 3 November 2020).

Delta-EE. 2017. Gas engines vs. Gas turbines – who will win the decentralized power generation race?. [webinar]. Available online: <https://www.delta-ee.com/webinars> (retrieved 28 July 2017).

Ekströms Värmetekniska. 2020. [www-page]. Available online: <https://ekstromsvarme.se/en/products/finnedtubes> (accessed

EPA. 2017. Section 2. Technology Characterization – Reciprocating Internal Combustion Engines. p. 2-1–2-27. In U.S. Environmental Protection Agency. 2017. Catalog of CHP Technologies. U.S. Environmental Protection Agency. Available online: <https://www.epa.gov/chp/catalog-chp-technologies> (retrieved 5 December 2018).

Flexim. 2010. User Manual for FLUXUS F601 UMFLUXUS_F6V4-0EN. [manual].

Federal Ministry for Economic Affairs and Energy. [www-page]. Available online: <https://www.bmwi.de/Redaktion/EN/Artikel/Energy/modern-power-plant-technologies.html> (accessed 4 December 2020).

García Pérez, M. 2016. Modeling the effects of unsteady flow patterns on the fireside ash fouling in tube arrays of kraft and coal-fired boilers. Doctoral dissertation. Lappeenranta University of Technology. ISBN 978-952-335-001-4.

Heat Management. 2020. Infrasound soot cleaning system. [brochure]. Available online: <https://www.heatmanage.com/wp-content/uploads/2018/11/2017-11-29-Heat-Management-LAND-broschyr-web.pdf> (retrieved 6 November 2020).

Jameel, M. I., Cormack, D. E., Tran, H. & Moskal, T. E. 1994. Sootblower optimization Part 1: Fundamental hydrodynamics of a sootblower nozzle and jet. 1994. *Tappi Journal*, vol. 77: 5, p. 135–142.

Kakko, M. 2017. The effect of the geometric parameters to the thermal-hydraulic dimensioning of a H-type finned tube heat exchanger. Master's thesis. Tampere University of Technology.

Kaliazine, A., Cormack, D. E., Ebrahimi-Sabet, A. & Train, H. 1998. The Mechanics of Deposit Removal in Kraft Recovery Boilers. *Journal of Pulp and Paper Science*, vol. 25: 12, p. 418–424.

Kaliazine, A, Cormack, D. E, Tran, H. & Jameel, I. 2006. Feasibility of using low pressure steam for sootblowing. *Pulp & Paper Canada*, 107: 4, p. 34–38.

Kaushik, M. 2019. *Theoretical and Experimental Aerodynamics*. Singapore: Springer Singapore Pte. Limited. p. 511. ISBN 978-981-13-1678-4.

Kern, D. Q. & Seaton, R. A. 1959. A Theoretical Analysis of Thermal Surface Fouling. *British Chemical Engineering*, vol. 4: 5, p. 258–262.

Kim, Y. M., Sohn, J. L. & Yoon, E. S. 2017. Supercritical CO₂ Rankine cycles for waste heat recovery from gas turbine. *Energy*, vol. 118, p. 893–905. ISSN 0360-5442.

Kockum Sonics. 2008. Sonic cleaning for Power- and Heatingplants. [brochure]. Available online: https://www.kockumation.com/Portals/kockumation/Documents/Industry/Sonic%20Cleaning_8sidA4web.pdf?ver=2016-08-26-140256-230 (retrieved 15 August 2020).

Kockum Sonics. Sonoforce® IKT 230GD/170. [brochure]. Available online: <https://www.kockumation.com/Portals/kockumation/Documents/Marine/Insonex/KSI627US%20IKT230-170.pdf?ver=2016-08-25-164333-117> (retrieved 15 August 2020).

Luoti, S. 2020. Business Development Manager, Alfa Laval Aalborg Oy. Rauma. Interview November 2020.

Läiskä, P. 2018. General Manager, Alfa Laval Aalborg Oy. Rauma. Interview June 2018.

Marner, W. J. & Suito J. W. 1983. A Survey of Gas-Side Fouling in Industrial Heat-Transfer Equipment.

Moskal, T. E. 1996. Overlooked moisture sources cause sootblower-induced tube erosion. *Pulp & paper*, vol. 70: 11, p. 91–92.

Müller-Steinhagen, H. 2010. C4 Fouling of Heat Exchanger Surfaces. p. 79–104. In Verein Deutscher Ingenieure & VDI-Gesellschaft Verfahrenstechnik und Chemieingenieurwesen (ed.). 2010. VDI Heat Atlas. 2nd edition. Berlin: Springer. 1585 p. ISBN 978-3-540-77877-6.

Müller-Steinhagen, H. 2011. Heat Transfer Fouling: 50 Years After the Kern and Seaton Model. *Heat Transfer Engineering*, vol. 32: 1, p. 1–13. ISSN 1521-0537.

Mäkelä, I. 2019. Calculation comparison of waste heat recovery boiler dimensioning tools for gas turbine application. Master's thesis. Lappeenranta-Lahti University of Technology LUT.

Paz, C., Suárez, E., Eirís, A. & Porteiro, J. 2013. Development of a Predictive CFD Fouling Model for Diesel Engine Exhaust Gas Systems. *Heat Transfer Engineering*, vol. 34: 8–9, p. 674–682. ISSN 1521-0537.

Pophali, A., Emami, B., Bussman, M. & Tran, H. 2013. Studies on sootblower jet dynamics and ash deposit removal in industrial boilers. *Fuel Processing Technology*, vol. 105, p. 69–76. ISSN 0378-3820.

Power Engineering International. 2017. MAN launches 26 MW diesel engine. Available online: <https://www.powerengineeringint.com/articles/decentralized-energy/2017/09/man-launches-26-mw-diesel-engine.html> (accessed 13 December 2018).

Pöyry. 2013. Memo - Stack gas calculation. Alfa Laval Aalborg Oy intranet: Access rights needed. (accessed 13 December 2018).

Rao, A. D. 2012. Combined Cycle Systems for Near-Zero Emission Power Generation. 1st edition. Philadelphia: Woodhead Pub. ISBN 1-62870-370-9.

Schimmoller, B. K. 1999. Tuning in to acoustic. *Power Engineering (Barrington, Ill.)*, vol. 103: 7, p. 18–26.

Vakkilainen, E. K. 2016. *Steam Generation from Biomass: Construction and Design of Large Boilers*. Oxford: Elsevier Science & Technology. ISBN 012804389X.

Wojnar, W. 2013. Erosion of heat exchangers due to sootblowing. *Engineering Failure Analysis*, vol. 33, p. 473–489. ISSN 1350-6307.

Wärtsilä. 2015. Flexicycle™ power plants. [brochure]. Available online: <http://cdn.wartsila.com/docs/default-source/Power-Plants-documents/downloads/brochures/flexicycle-power-plants-2015.pdf> (retrieved 5 May 2018).

Wärtsilä. 2017. Combined heat and power & trigeneration solutions. [brochure].

Wärtsilä. 2018. Wärtsilä [www-page]. Available online: <https://www.wartsila.com/energy/learning-center/technical-comparisons/combustion-engine-vs-gas-turbine-part-load-efficiency-and-flexibility> (accessed 8 December 2018).